



Performance Assessment of Advanced Digital Measurement and Protection Systems

*Final Project Report
Part II*

Power Systems Engineering Research Center

*A National Science Foundation
Industry/University Cooperative Research Center
since 1996*





Power Systems Engineering Research Center

Performance Assessment of Advanced Digital Measurement and Protection Systems

Final Report for PSERC Project T-22 Part II

**Lead Investigator:
Mladen Kezunovic**

**Graduate Students:
Levi Portillo
Bogdan Naodovic**

Texas A&M University

PSERC Publication 06-22

July 2006

Information about this project

For information about this project contact:

Mladen Kezunovic, Ph.D.
Texas A&M University
Department of Electrical Engineering
College Station, TX 77843
Tel: 979-845-7509
Fax: 979-845-9887
Email: kezunov@ece.tamu.edu

Power Systems Engineering Research Center

This is a project report from the Power Systems Engineering Research Center (PSERC). PSERC is a multi-university center conducting research on challenges facing a restructuring electric power industry and educating the next generation of power engineers. More information about PSERC can be found at the Center's website: <http://www.pserc.org>.

For additional information, contact:

Power Systems Engineering Research Center
Arizona State University
Department of Electrical Engineering
Ira A. Fulton School of Engineering
Phone: (480) 965-1879
Fax: (480) 965-0745

Notice Concerning Copyright Material

PSERC members are given permission to copy without fee all or part of this publication for internal use if appropriate attribution is given to this document as the source material. This report is available for downloading from the PSERC website.

Acknowledgements

This is Part II of the final report on the PSERC project “Performance Assessment of Advanced Digital Measurement and Protection Systems (T-22).” We express our appreciation for the support provided by PSERC's industrial members and by the National Science Foundation under grant NSF EEC-0002917, awarded to Texas A&M University and received under the Industry / University Cooperative Research Center program.

We also thank the PSERC research project industry advisors for their technical advice. We especially thank AEP staff (Dale Krummen, John Mandeville, Dave Bernert, and Joon Park) for their support with field data, and NxtPhase staff (Dylan Stewart, Farnoosh Rahmatian and Patrick Chavez) for their support with technical information about optical sensors.

Executive Summary

Recently, optical voltage and current transducers, often called Optical Voltage Transformers (OVTs) and Optical Current Transformers (OCTs) respectively, have become readily available. The signals from OCTs and OVTs can be communicated to a control room through fiber optic cables. In the control room, the signals may supply a digital device, such as a relay, an energy metering system, or a power quality meter. This all-digital system may be more advantageous than conventional systems that use magnetic Current Transformers (CTs) and Potential Transformers (PTs). PTs include both Voltage Transformers and Coupling Capacitor Voltage Transformers. The optical transformers may provide improved transient response (due to a wider frequency band), improved dynamic range, and higher accuracy. This research project has sought to explore and quantify the advantages of an integrated measurement and protection system using OCTs and OVTs over a traditional system that uses conventional magnetic CTs and PTs.

The comparison of the two systems was done by evaluating their relative performance when supporting the functions of protection, revenue metering, and power quality metering. This indirect approach was used, in part, because direct input/output evaluation of the optical transformers relative to magnetic transformers was not possible. The necessary input signals were not accessible in the field trials (as in most field applications) due to the high cost of retrofitting existing instrument transformers with a high accuracy referent sensor that can measure the input signals. More generally, comparison of component characteristics alone does not necessarily indicate how different component characteristics affect the performance of the functions served by those components. Hence, the approach of evaluating input/output relationships for the transformers was not pursued and instead the evaluation of the impact of different transformers on the performance of IEDs was undertaken instead. Performance indices for the functions of protection, revenue metering, and power quality metering were developed to compare the two systems quantitatively.

The indirect approach was carried out using a software model of an OCT that was developed through a series of tests performed on an actual OCT in a high power lab. Co-investigators from Arizona State University (ASU) conducted lab tests and developed the OCT model as described in a companion project report

This indirect approach has a number of advantages in comparing instrument transformer characteristics based on the performance of a system that uses only the outputs from the transformer models.

- Simulation environment (software) can be easily expanded to evaluate new instrument transformers using their models as the transformers become available on the market. It is also possible to incorporate different power network configurations and intelligent electric devices (IEDs)
- The modular nature of the simulation environment makes possible the use of historical field-recorded data from different sets of instrument transformers or IEDs.

- Numerical performance indices can be useful for evaluating performance of instrument transformers from different manufacturers

Due to the challenges in the field data collection during this project, analysis of field data could only be used on selected cases. For the cases analyzed, the following results were obtained:

- Higher accuracy of optical instrument transformers with respect to conventional instrument transformers did not translate into significant improvement in the performance of the power quality and/or revenue metering IED's.
- Wider frequency bandwidth of the optical instrument transformers considerably improved their relative performance for relaying and metering applications.
- Performance of protection IED's improved when fed with signals from optical current transformers. In almost all cases, the improved performance was due to the absence of conventional CT saturation. Not all of the conventional CT models tested experienced saturation up to the level that would cause misoperation of protection IED. This suggests that the problem of saturation on protection IED performance can be avoided even when using conventional CTs by proper instrument transformer sizing.

The results suggest that detailed engineering and economic analysis is required to determine the appropriateness of using an optical transformer system instead of a system with magnetic CTs and PTs. The decision to upgrade to an optical system will depend upon the performance of the conventional systems, performance of new optical transformers (in our case represented by software) models and on the objectives sought in making the upgrade.

Table of Contents

1. Introduction.....	1
2. Literature Review and State-Of-The-Art Report	2
2.1 Introduction.....	2
2.2 Characteristics of Conventional Instrument Transformers	2
2.2.1 Designs	2
2.2.1.1 Current Transformers.....	2
2.2.1.2 Voltage Transformers	3
2.2.2 Accuracy.....	5
2.2.2.1 Revenue Metering Accuracy Class.....	5
2.2.2.2 Relaying Accuracy Class	6
2.2.3 Frequency Bandwidth.....	6
2.2.3.1 Current Transformers.....	6
2.2.3.2 Voltage Transformers	6
2.2.4 Transient Response.....	7
2.2.4.1 Current Transformers.....	9
2.2.4.2 Voltage Transformers	10
2.3 Conclusion	13
3. Methodology for Assessment of the Benefit of Improved Instrument Transformer Performance Characteristics	14
3.1 Introduction.....	14
3.2 Evaluation Criteria.....	14
3.2.1 Indirect Evaluation	14
3.2.2 Evaluation of Intelligent Electronic Devices.....	15
3.2.3 Evaluation of a Measuring Algorithm.....	16
3.2.3.1 Time Responses Indices.....	16
3.2.3.2 Frequency Response Indices.....	17
3.2.4 Evaluation of a Decision-Making Algorithm.....	18
3.2.5 Use of the Criteria	20
3.3 Evaluation Methodology.....	21
3.3.1 Definition of Methodology.....	21
3.3.2 Exposure Signals	23

3.3.3	Evaluation Based on Simulation	25
3.3.4	Models Used in Simulations.....	25
3.3.4.1	Power Network	25
3.3.4.2	Current Transformer	26
3.3.4.3	Coupling-Capacitor Voltage Transformer	28
3.3.4.4	Overcurrent Protection Numerical Relay (Model A).....	29
3.3.4.5	Line Impedance Protection Numerical Relay (Model B)	30
3.3.4.6	Power Quality Meter (Model C).....	31
3.4	Conclusion	31
4.	Assessment of the Benefit of Higher Accuracy	32
4.1	Introduction.....	32
4.2	Scenarios	32
4.3	Evaluation Results	33
4.4	Assessment of Higher Accuracy.....	34
4.5	Conclusion	34
5.	Assessment of the Benefit of Wider Frequency Bandwidth	35
5.1	Introduction.....	35
5.2	Evaluation of Frequency Bandwidth	35
5.2.1	Scenarios	35
5.2.2	Evaluation Results.....	36
5.3	Assessment of Wider Frequency Bandwidth.....	36
5.4	Conclusion	37
6.	Assessment of the Benefit of Improved Transient Response	38
6.1	Introduction.....	38
6.2	Evaluation of Transient Response	38
6.2.1	Scenarios	38
6.2.2	Evaluation Results.....	39
6.2.2.1	IED Model A.....	40
6.2.2.2	IED Model B.....	44
6.3	Assessment of Improved Transient Response	45
6.3.1.1	IED Model A.....	45
6.3.1.2	IED Model B.....	46
6.4	Conclusion	47

7. Assessment Using Field Recorded Data	48
7.1 Introduction.....	48
7.2 Sources of Field Recorded Data	48
7.3 Evaluation of Transient Response	49
7.4 Evaluation of Accuracy	50
7.5 Conclusion	51
8. Conclusion	52
References.....	54
Appendix – Published Conference Papers	56

Table of Figures

Figure 2.1 Mounting of HV Current Transformer	3
Figure 2.2 Equivalent Circuit of a CCVT	4
Figure 2.3 Mounting of HV Coupling Capacitor Voltage Transformer	4
Figure 2.4 Frequency Response of a Current Transformer.....	7
Figure 2.5 Frequency Response of a Voltage Transformer.....	7
Figure 2.6 Frequency Response of CCVT	8
Figure 2.7 Primary Current and Electromagnetic Flux Density in the Core.....	8
Figure 2.8 Primary and Secondary Currents.....	10
Figure 2.9 Time-To-Saturation Curves.....	11
Figure 2.10 CCVT Subsidence Transient	11
Figure 2.11 Influence of FSC.....	12
Figure 3.1 Concept of Indirect Evaluation.....	15
Figure 3.2 Subfunctions of IED	15
Figure 3.3 Flowchart of Decision Making	16
Figure 3.4 Typical Time Response of a Measuring Algorithm	17
Figure 3.5 Ideal and Actual Response of Measuring Algorithm	18
Figure 3.6 Exposure Signals From a Fault Event	23
Figure 3.7 Steps of the Simulation Approach.....	25
Figure 3.8 Model of Power Network	26
Figure 3.9 Equivalent Circuit of Current Transformer Model.....	27
Figure 3.10 V-I Characteristics of Electromagnetic Core of a Current Transformer	28
Figure 3.11 Configurations of Coupling-Capacitor Voltage Transformers	28
Figure 4.1 Functional Elements and Flowchart of IED Model C	32
Figure 5.1 Functional Elements and Flowchart of IED Model C	35
Figure 6.1 Signals Associated with Abc-Phase-To-Ground Fault.....	41
Figure 6.2 Comparison of Performance Index t_{lmax}	42
Figure 7.1 Setup for Field Data Recording	49

Table of Tables

Table 2.1	Standard Accuracy Classes for Revenue Metering.....	5
Table 2.2	Secondary Terminal Voltages and Associated Standard Burdens	6
Table 3.1	Performance Indices for the Time Response of Measuring Algorithm	17
Table 3.2	Performance Indices for the Frequency Response of Measuring Algorithm....	18
Table 3.3	Performance Indices - Decision Making Algorithm	19
Table 3.4	Additional Performance Indices - Decision Making Algorithm	20
Table 3.5	Parameters of Equivalent Circuit of Current Transformer Model	27
Table 3.6	Parameters of Current Transformer Models	27
Table 3.7	Parameters of Coupling-Capacitor Voltage Transformer Models	29
Table 3.8	IED and Models	29
Table 4.1	Simulation Scenario, IED Model C, Voltage Sag/Swell.....	33
Table 4.2	Simulation Scenario, IED Model C, Flicker	33
Table 4.3	Sag and Swell Characterization	34
Table 4.4	Flicker Characterization	34
Table 5.1	Simulation Scenario, IED Model C, Harmonics.....	36
Table 5.2	Simulation Scenario, IED Model C, Transients.....	36
Table 5.3	Harmonics Characterization.....	36
Table 5.4	Transients Characterization.....	36
Table 6.1	Simulation Scenario, IED Model A	39
Table 6.2	Simulation Scenario, IED Model B	39
Table 6.3	Current Measuring Element, ABCG Fault.....	42
Table 6.4	Current Measuring Element, AG Fault	42
Table 6.5	Current Measuring Element, BC Fault.....	42
Table 6.6	Voltage Measuring Element, ABCG Fault	43
Table 6.7	Voltage Measuring Element, AG Fault.....	43
Table 6.8	Voltage Measuring Element, BC Fault	43
Table 6.9	Overcurrent Decision Element, ABCG Fault.....	43
Table 6.10	Overcurrent Decision Element, AG Fault.....	44
Table 6.11	Overcurrent Decision Element, BC Fault	44
Table 6.12	Distance Decision Element, ABCG Fault.....	44
Table 6.13	Distance Decision Element, AG Fault	45
Table 6.14	Distance Decision Element, BC Fault.....	45
Table 7.1	Relay – Field Recorded Data	50
Table 7.2	Power Quality Performance - 16 Recorded Sags.....	50

1. Introduction

This report presents results from an evaluation of instrument transformer performance characteristics based on modeling and simulation. The tasks aimed at this effort were defined in the statement of work for project titled, "Performance Assessment of Advanced Digital Measurement and Protection Systems". The tasks were defined as:

- Literature review and state-of-the-art report
- Assessment of the benefit of higher accuracy
- Assessment of the benefit of wider frequency band and wide dynamic range
- Assessment of the benefit of improved transient response on system control
- Assessment of operation data provided by AEP

This report presents evaluation criteria, methodology and implementation of the methodology. The methodology was implemented through extensive simulation software. Simulation environment encompasses models of all the equipment involved in the evaluation. A model of the optical current transducer was developed by Arizona State University and has been included in this report. A model of the optical voltage transducer was not available. Therefore, it was not possible to evaluate performance of the optical VT model.

2. Literature Review and State-Of-The-Art Report

2.1 Introduction

The first objective addresses the current state-of-the-art in the field of instrument transformers. Certain shortcomings are inherent to conventional instrument transformer designs (electromagnetic and coupling capacitor). Theoretical research and field application has shown that the mentioned shortcomings may be sufficient to cause unexpected performance of the protection, control, and monitoring subsystem applications in the electric power systems. In order to understand the shortcomings and mechanism of their influence, characteristics of conventional instrument transformer should be reviewed

2.2 Characteristics of Conventional Instrument Transformers

Characteristics of the conventional instrument transformer designs (electromagnetic and coupling-capacitor) are well understood and described in the available literature [1], [2] and [3]. Operating principles are described in [1] and [2]. Historical background is given in [3]. The characteristics that define instrument transformer behavior are:

- Accuracy
- Frequency Bandwidth
- Transient Response

Accuracy is a measure of difference between the original power network current and voltage signals and scaled-down replicas. Transient response is behavior of instrument transformers during transient power network conditions. Frequency bandwidth is a measure of maximum frequency range that can be occupied by the original power network signals to still be scaled-down correctly. The typical instrument transformer designs and characteristics are described in the sections to follow.

2.2.1 Designs

Instrument transformers are available in a number of types and can be connected in a number of ways to provide the required quantities.

2.2.1.1 Current Transformers

Current transformers are available primarily in two types: bushing and wound. Bushing transformers are usually less expensive than wound transformers, but they have lower accuracy. They are often used for relaying because of their favorable cost and because their accuracy is often adequate for relay applications. Bushing transformers are conveniently located in the bushings of power transformers and dead-tank circuit breakers, and therefore take up no appreciable space in the substation. Dead-tank circuit breakers are the preferred type of breakers in the United States, which means that they are present in much larger number than live-tank circuit breakers. Different between dead-

tank and live-tank breakers is that former ones are grounded, while the later ones are not. Because of this, live-tank breakers demand stand alone CT, i.e. CT cannot be simply mounted on the breaker; they have to be physically separated. This translates into CT for live-tank breakers being constructed in form of tall columns (consisting of insulators), isolating them from the ground. These CT are usually submerged in oil.

Bushing transformers are mounted in the bushing of dead-tank breakers. They are designed with a core encircling an insulating column through which the primary current lead connects to the bushing. This means that the diameter of the core is relatively large, giving a large mean magnetic path length compared to other types. The bushing transformer also has only one primary turn, namely, the metallic connection through the center of the bushing. To compensate for the long path length and minimum primary turn condition, the cross-sectional area of iron is increased. This has the advantage for relaying that the bushing transformer tends to be more accurate than wound transformer at large multiples of secondary current rating. The bushing transformer, however, is less accurate at low currents because of its large exciting current. This makes the bushing transformer a poor choice for applications such as metering, which requires good accuracy at nominal currents.



Fig. 2.1: Mounting of HV Current Transformer

2.2.1.2 Voltage Transformers

There are two types of voltage measuring devices. They are: 1) electromagnetic voltage transformer (VT), which is a two-winding transformer, 2) coupling-capacitor voltage transformer (CCVT), which contains a capacitive voltage divider.

The electromagnetic transformer is much like a conventional power transformer except that it is designed for a small constant load and hence cooling is not as important as accuracy. The coupling-capacitor device is a series stack of capacitors with the secondary tap taken from the last unit, which is called the auxiliary capacitor.

The equivalent circuit of a coupling-capacitor transformer is shown in Figure 2.2 (ZB represents the transformer burden). The equivalent reactance of this circuit is defined by equation:

$$X_L = \frac{X_{C1} \cdot X_{C2}}{X_{C1} + X_{C2}}$$

This reactance is adjusted to bring the applied voltage and the tapped voltage in phase, in which case the device is called a resonant coupling-capacitor transformer. Since the bottom capacitor is much larger than the top capacitor, i.e.

$$X_{C1} \ll X_{C2}$$

It follows that practically

$$X_L \cong X_{C2}$$

Coupling-capacitor transformers are usually designed to reduce the transmission-level voltage V_S to a safe metering level V_B by a capacitive voltage divider, although an electromagnetic transformer may be needed to further reduce the voltage to IED voltages, usually 67 V line-to-neutral (115 V line-to-line).

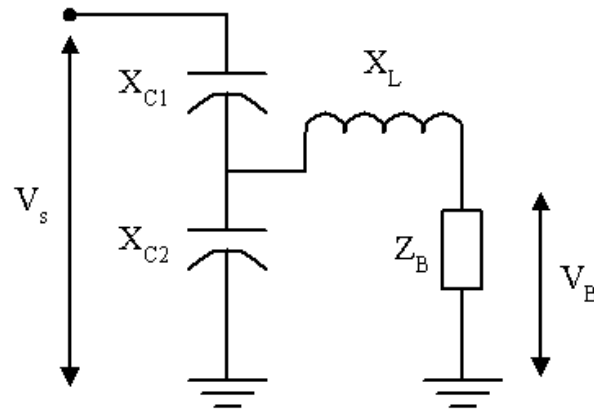


Fig. 2.2: Equivalent Circuit of a CCVT



Fig. 2.3: Mounting of HV Coupling Capacitor Voltage Transformer

2.2.2 Accuracy

There are two accuracy-rating classes for conventional instrument transformers defined in the IEEE standard [4]:

- Revenue Metering Class
- Relaying Class

The definitions are based around the term transformer correction factor (TCF) [4]. TCF is the ratio of the true watts or watt-hours to the measured secondary watts or watt-hours, divided by the marked ratio. TCF is equal to the ratio correction factor multiplied by the phase angle correction factor for a specified primary circuit power factor. Ratio correction factor (RCF) is the ratio of the true ratio to the marked ratio. True ratio is the ratio of the root-mean-square (RMS) primary voltage or current to the RMS secondary voltage or current under specified conditions. Phase angle correction factor (PACF) is the ratio of the true power factor to the measured power factor. It is a function of both the phase angles of the instrument transformers and the power factor of the primary circuit being measured.

2.2.2.1 Revenue Metering Accuracy Class

Accuracy classes for revenue metering are based on the requirement that the TCF of the voltage transformer or of the current transformer will be within specified limits when the power factor (lagging), of the metered load has any value from 0.6 to 1.0, under specified conditions as follows:

- For current transformers, at the specified standard burden at 10 percent and at 100 percent of rated primary current (also at the current corresponding to the rating factor (RF) if it is greater than 1.0). The accuracy class at a lower standard burden is not necessarily the same as at the specified standard burden.
- For voltage transformers, for any burden in volt-amperes from zero to the specified standard burden, at the specified standard burden power factor and at any voltage from 90 percent to 110 percent of the rated voltage. The accuracy class at a lower standard burden of different power factor is not necessarily the same as at the specified standard burden.

The limits for the revenue metering accuracy classes are given in Table 2.1.

Table 2.1: Standard Accuracy Classes for Revenue Metering

CLASS	VT		CT			
			100% rated		10% rated	
	Min	Max	Min	Max	Min	Max
0.3	0.997	1.003	0.997	1.003	0.994	1.006
0.6	0.994	1.006	0.994	1.006	0.988	1.012
0.12	0.988	1.012	0.988	1.012	0.976	1.024

2.2.2.2 Relaying Accuracy Class

For relaying accuracy ratings, the ratio correction will not exceed 1 percent. Relaying accuracy ratings will be designated by a classification and a secondary terminal voltage rating as follows:

C, K, or T classification. C or K classification covers current transformers in which the leakage flux in the core of the transformer does not have an appreciable effect on the ratio or ratios within the limits of current and burden outlined in this item, so that the ratio can be calculated in accordance with the algebraic method (given in [4]). Current transformers with K classification will have a knee-point voltage at least 70 percent of the secondary terminal voltage rating. T classification covers current transformers in which the leakage flux in the core of the transformer has an appreciable effect on the ratio within the limits specified in item 2. An appreciable effect is defined as a 1 percent difference between the values of actual ratio correction and the ratio correction calculated in accordance with the algebraic method.

Secondary terminal voltage rating. This is the voltage the transformer will deliver to a standard burden at 20 times rated secondary current without exceeding 10 percent ratio correction. Furthermore, the ratio correction will be limited to 10 percent at any current from 1 to 20 times rated secondary current at the standard burden or any lower standard burden used for secondary terminal voltage ratings.

The voltage ratings and their associated burdens are as given in Table 2.2.

Table 2.2: Secondary Terminal Voltages and Associated Standard Burdens

SECONDARY TERMINAL VOLTAGE	10	20	50	100	200	400	800
STANDARD BURDEN	B-0.1	B-0.2	B-0.5	B-1	B-2	B-4	B-8

2.2.3 Frequency Bandwidth

2.2.3.1 Current Transformers

Typical frequency response of a conventional CT is given in Figure 2.4 [5]. As can be seen in the figure, the transformer ratio is constants over a wide frequency range. The phase angle is also constant and has zero value. For practical purposes CT can be regarded as not having influence on the spectral content of the input signal under condition that electromagnetic flux in the core is in the linear region. In the case the flux goes out of the linear region, the change of the frequency response is hard to predict. This situation is discussed in the section 2.5.

Based on frequency response of CTs, it follows that their frequency bandwidth is not limited for all practical purposes.

2.2.3.2 Voltage Transformers

Typical frequency response of an EM voltage transformer is given in Figure 2.5 [5]. As can be seen in the figure, the transformer ratio varies significantly over wide frequency range. The phase angle also shows significant variations. Most notable sources of transformer ratio frequency dependability are: 1) stray capacitances of the primary and secondary windings, 2) stray capacitances between primary and secondary windings [6].

Typical frequency response of a coupling-capacitor voltage transformer is given in Figure 2.6 [5]. Figure also shows variations of the frequency response with the change

of various capacitances (where CC is compensating inductor stray capacitance, CP is step down transformer primary winding stray capacitance).

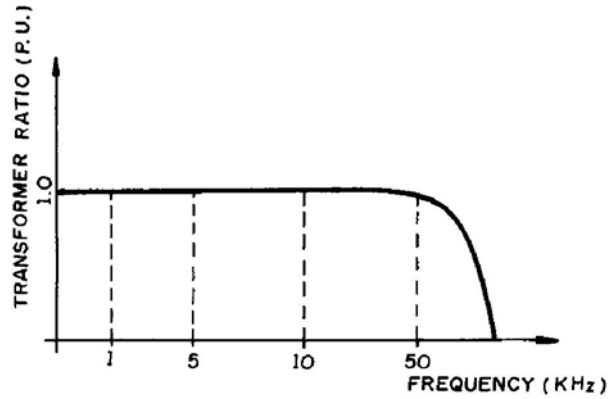


Fig. 2.4: Frequency Response of a Current Transformer [5]

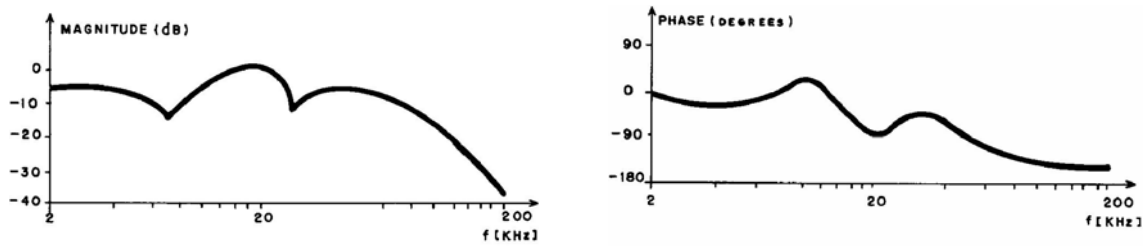


Fig. 2.5: Frequency Response of a Voltage Transformer [5]

Similarly as with voltage transformers, the transformer frequency response varies significantly over wider frequency range. The phase angle also shows significant variations. Most notable sources of transformer ratio frequency dependability are the same as with voltage transformers. Another factor that influences frequency response of CCVTs is the ferroresonance suppression circuit [7]. This circuit acts as a band pass filter, with center frequency at 60 Hz. More details on impact of this circuit are given in the section that deals with transient response of ITs.

Frequency bandwidth of voltage VTs and CCVTs is limited. The exact limit depends on the definition of the bandwidth.

2.2.4 Transient Response

The mentioned standard [4] addresses instrument transformer behavior only during the steady state and symmetrical fault power system conditions. Since behavior of instrument transformers may be significantly different for transient conditions, transient response of conventional instrument transformers has been studied. Transient response of a current transformer refers to the ability of a current transformer to handle the DC component in an asymmetrical current waveform [8]. Transient response of a voltage transformer refers

to the ability of a voltage transformer to control its tendency to create extraneous frequencies in the output [9].

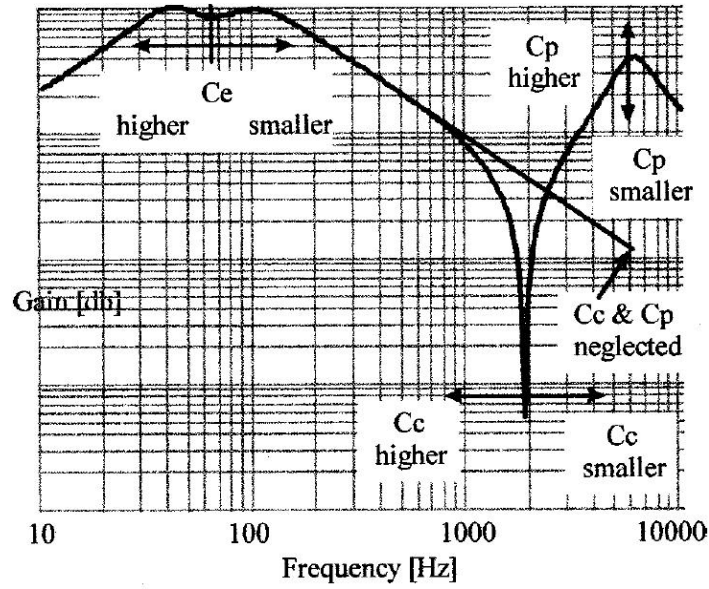
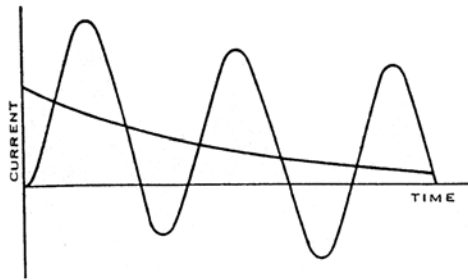
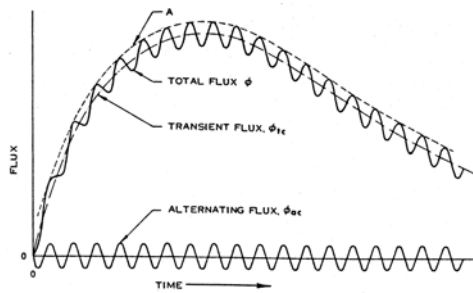


Fig. 2.6: Frequency Response of CCVT [6]



(a) Current Density



(b) Flux Density

Fig. 2.7: Primary Current and Electromagnetic Flux Density in the Core [8]

2.2.4.1 Current Transformers

Saturation of the electromagnetic core is the single factor that shapes the current transformer transient response the most. Saturation may lead to signal distortions in the current transformer output. Distortion occurs whenever the core flux density enters the region of saturation. The factors influencing the core flux density are: 1) physical parameters of the current transformer, 2) magnitude, duration and waveform of the primary current signal, 3) nature of the secondary burden [8]. Saturation of the electromagnetic core can be initiated by excessive symmetrical fault currents as well as by lower magnitude asymmetrical (offset) fault currents.

The fully offset fault current is shown in Figure 2.7(a). When a fully offset current is impressed on the primary of a current transformer, it will induce core flux density as shown in Figure 2.7(b) (assuming a resistive current transformer burden without loss of generality).

There are two components of the total flux Φ . Alternating flux Φ_{ac} is the flux induced by the fundamental frequency component of the fault current. Transient flux Φ_{tc} is the flux induced by the DC component of the fault current. The variation of the transient flux Φ_{tc} is a function of both the primary and the secondary current transformer circuit time constants. The primary current transformer circuit constant is defined by the power network section to which the current transformer is connected. The secondary current transformer circuit time constant is defined by: 1) current transformer secondary leakage impedance, 2) current transformer secondary winding impedance, 3) burden impedance. The current transformer secondary leakage impedance can usually be neglected and the current transformer secondary winding impedance is usually combined with the burden impedance to form the total burden. The dependence of the level of the saturation on the total burden is shown in Figure 2.8 [8]. The figure presents comparison between the secondary and the primary (referred to the secondary) current of a 1200:5 current transformer subjected to a fully offset current of 24000 A (20 time the rated value). In Figure 2.8(a) the current transformer is connected to the burden of $Z_1 = (2.6 + j0) \Omega$, while in Figure 2.8(b) the burden is $Z_2 = (1.6 + j0) \Omega$.

It can be seen in Figure 2.8 that distortion begins certain amount of time after the fault inception. The notion of the time-to-saturation is introduced as a measure of the mentioned amount of time. The time-to-saturation is defined as the time period starting after the fault inception during which the secondary current is a faithful replica of the primary current. The time-to-saturation can be determined analytically given the power system parameters. A more practical approach is to generate a set of generalized curves that can be used for direct reading of the time-to-saturation. A set of such curves can be found in [8]. A typical set of curves is given in Figure 2.9.

The set of curves is based on the current transformer primary circuit time constant $T_1 = 0.02$ sec. Different set of curves can be obtained for a different time constant T_1 . The set contains curves corresponding to the current transformer secondary circuit time constant T_2 ranging from 0.1 sec to 10 sec. The determination of the time-to-saturation is based on the saturation factor K_s . The factor can be calculated as:

$$K_s = \frac{V_x N_2}{I_1 R_2} = \frac{\omega T_1 T_2}{T_1 - T_2} \left(e^{-\frac{t}{T_2}} - e^{-\frac{t}{T_1}} \right) + 1$$

Where:

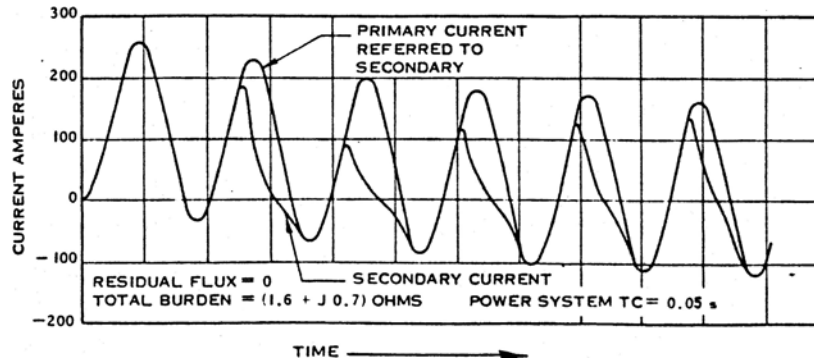
V_x is RMS saturation voltage

N_2 is the number of secondary windings

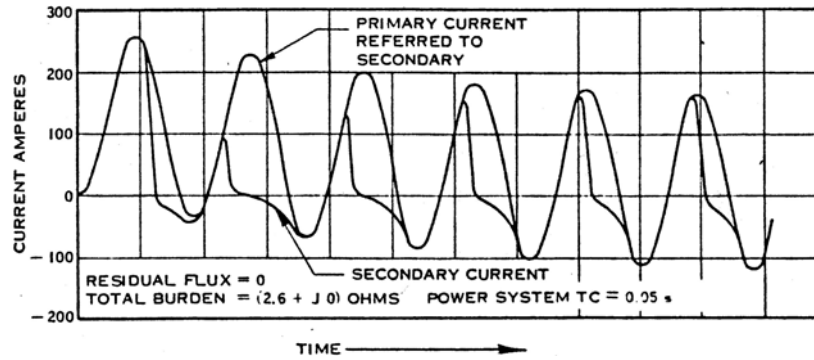
I_1 is the primary current magnitude

R_2 is the resistance of total secondary burden (winding plus external resistance)

ω is $2\pi \cdot 60$ rad



(a) Low Burden



(b) High Burden

Fig. 2.8: Primary and Secondary Currents [8]

2.2.4.2 Voltage Transformers

The transient response of electromagnetic voltage transformers and coupling capacitor voltage transformers depends on several distinct phenomena taking place in the primary network, such as sudden decrease of voltage at the transformer terminals due to a fault or sudden overvoltages on the sound phases during line to ground faults on the network [6].

Sudden decrease of voltage at the primary terminals could generate internal oscillations in the windings of electromagnetic voltage transformers, which creates a high frequency on the secondary side.

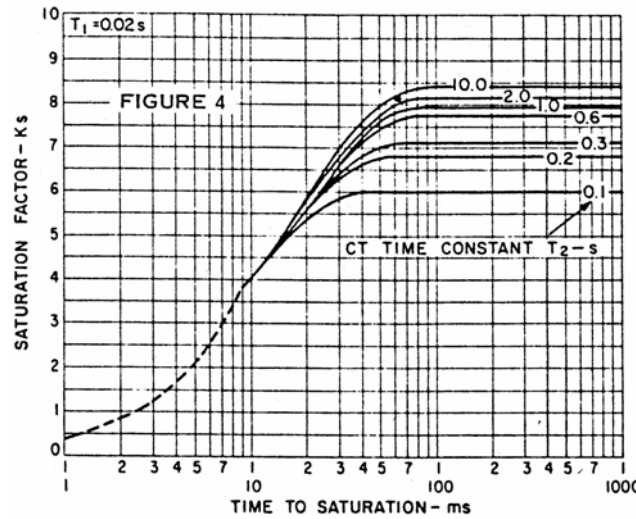


Fig. 2.9: Time-To-Saturation Curves [8]

These high frequency oscillations are typically damped within 15–20 ms. In the case of coupling-capacitor voltage transformer, energy stored in the capacitive and inductive elements of the device generate transients with low frequency of aperiodic character which could last up to 100 ms. Sudden increase of voltage at the primary terminals of electromagnetic voltage transformers could cause saturation of the magnetic core.

The transient response of coupling-capacitor voltage transformers is studied in reference [9]. The study investigates the subsidence transient. The subsidence transient is the factor that influences the voltage transformer transient response the most. The subsidence transient is defined as error voltage appearing at the output terminals of a coupling-capacitor voltage transformer resulting from a sudden and significant drop in the primary voltage. The transient can be classified as belonging to one of the three classes: 1) unidirectional, 2) oscillatory, $f > 60$ Hz, 3) oscillatory, $f < 60$ Hz (see Figure 2.10). The two factors that influence the subsidence transient the most are coupling-capacitor voltage transformer burden and coupling-capacitor voltage transformer design.

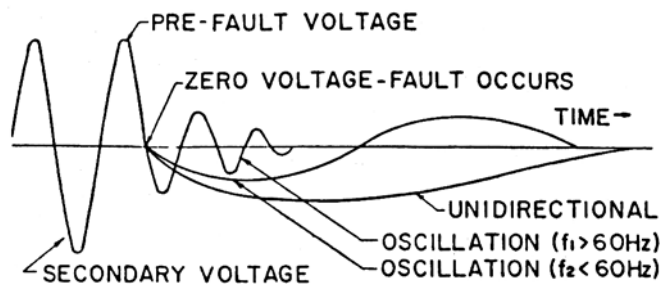


Fig. 2.10: CCVT Subsidence Transient [9]

Elements of the coupling-capacitor voltage transformer burden that influence the subsidence transient are: 1) burden magnitude, 2) burden power factor, 3) composition and connection of the burden. Considering the burden magnitude, most of the coupling-capacitor voltage transformer designs give smaller subsidence transient for burdens of the lower magnitude than the rated. Considering the burden power factor, the subsidence transient becomes greater as the power factor decreases, either lagging or leading. Considering the composition and connection of the burden, the following general remarks hold [9]: 1) high Q inductive elements in the burden tend to make the subsidence transient greater, 2) surge capacitors have only a minor effect on the subsidence transient, 3) series RL burdens for the same volt-ampere and power factor give smaller subsidence transient than parallel RL burdens.

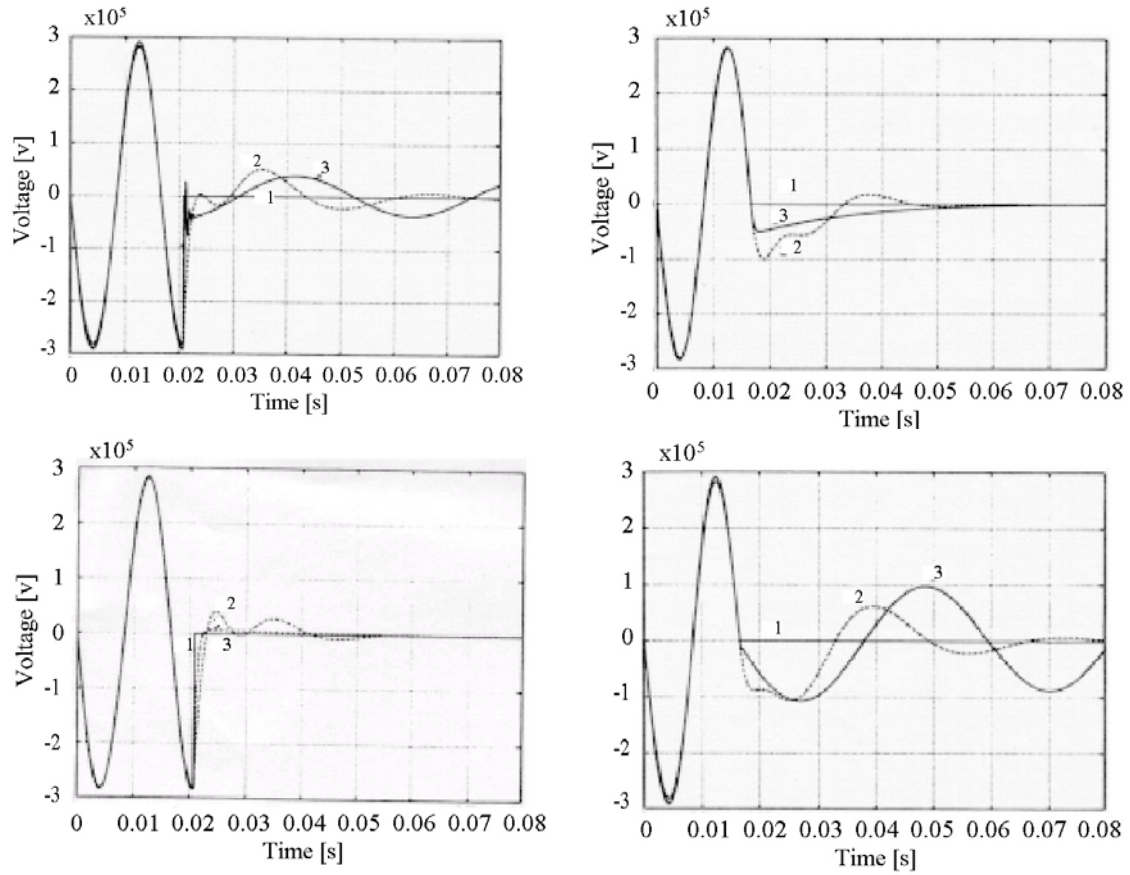


Fig. 2.11(a-d): Influence of FSC (a-b) resistive burden (fault initialization at zero and maximum voltage. (c-d) inductive burden (fault initialization at zero and maximum voltage)

Another aspect of the transient response of coupling-capacitor voltage transformers is the impact of ferroresonance suppression circuit (FSC). This phenomenon is studied in the reference [7]. The ferroresonance is usually characterized by over voltage oscillations and distorted waveforms of current and voltage. The oscillations are mostly of subharmonic frequencies, although harmonic and even fundamental

frequencies may also be present. In order to prevent negative impact of the ferroresonance, all coupling-capacitor voltage transformers contain a ferroresonance suppression circuit, which is connected on the secondary side. FSC designs, according to their status during the transformer operation, can be divided into two main operational modes [7]:

- FSC in an active operation mode consists of capacitors and iron core inductors connected in parallel and tuned to the fundamental frequency. They are permanently connected on the secondary side and affect the transformer transient response.
- FSC in a passive operation mode consists of a resistor connected on the secondary side. This resistor can be permanently connected. Another option is to have a gap or an electronic circuit connected in series with the resistor, which are activated whenever an over voltage occurs. Such an FSC does not affect transformers transient response unless an over voltage occurs.

Simulation of voltage collapse may be used as a typical example of FSC influence on the transformer transient response. The simulation results shown here are based on and FSC in active operation mode. The simulation of voltage collapse has been done using EMTP for a resistive and inductive burden of 100Ω . Fault initiations were at the voltage zero and maximum value. The influence of the FSC is shown in Figure 2.11 (note: 1 denotes primary voltage, 2 denotes secondary voltage with FSC, referred to primary, 3 denotes secondary voltage without FSC, referred to primary).

2.3 Conclusion

In this section, characteristics of typical conventional CT and VT/CCVT designs were described from the standpoint of protection system. Advantages and disadvantages of some designs over others were addressed.

Three most notable instrument transformer (IT) characteristics - accuracy, frequency bandwidth and transient response, were investigated. It was shown that all three characteristics can lead to distortions in secondary waveforms that are caused by IT design characteristics. Main source of distortions with CT is saturation. Main source of distortions with VT/CCVT is subsidence transient. Causes and mechanisms of mentioned distortions were discussed. Means of lessening their impact were also addressed.

The conclusion is that the impact of characteristics of the design of conventional IT on distortions is significant. When power system conditions are adverse, output signal can be significantly different from the ideal scaled-down version of input signal.

3. Methodology for Assessment of the Benefit of Improved Instrument Transformer Performance Characteristics

3.1 Introduction

This section presents evaluation criteria, methodology and implementation of the methodology. Methodology was implemented through extensive simulation software. Simulation environment encompasses models of all the involved equipment. Only a model of an optical current transformer was available during creation of results for this final report. It was not possible to evaluate the optical voltage transformers. However, evaluation criteria and methodology are expandable. Models of optical voltage transformers can be readily integrated into simulation software in order to produce any results in the future. No further action is necessary beyond integration of models. To demonstrate contribution of the simulation environment to the project outcome, detailed evaluation of transient response of several conventional instrument transformers is presented, as an example of results.

3.2 Evaluation Criteria

Criteria for evaluation of instrument transformers are presented in this section. First, concept of indirect evaluation is explained. Next, functional elements of power equipment are described as background for the criteria. The criteria are defined afterwards.

3.2.1 Indirect Evaluation

Evaluation of the influence is done by observing behavior of control, monitoring and protection equipment when supplied with input signals coming from outputs of a particular instrument transformer under investigation. Observation of behavior means recording available output signals from the equipment and analyzing them afterwards. Objective of the analysis is extraction of performance indices. Performance indices characterize behavior of power system equipment. There are two possible approaches to evaluation:

- Direct evaluation
- Indirect evaluation

Direct approach consists of comparing signals recorded on the primary side (of instrument transformers) with signals recorded on the secondary side. Primary side signals are regarded as referent signals. Since it is assumed (in this report) that signals from primary side are not available, an indirect approach for evaluation is chosen. Indirect evaluation defines criteria in the context of protection, control and monitoring functions. The concept of indirect approach is illustrated in Figure 3.1.

Indirect evaluation allows comparison of behavior of a device (representing monitoring, control or protection equipment) when it is exposed to signals coming from different instrument transformers. Mentioned concept mitigates the problem of absence of referent (primary side) signals by assuming that differences in behavior of a device are

due solely to different impacts of instrument transformers. This assumption does not negate that devices can malfunction for other reasons. The assumption means that focus of this report is the influence of instrument transformer on the devices, and possible miss-operations associated with the influence.

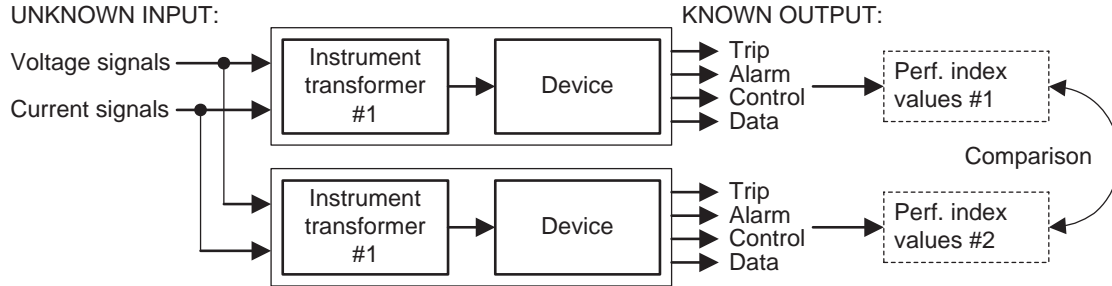


Fig. 3.1: Concept of Indirect Evaluation

3.2.2 Evaluation of Intelligent Electronic Devices

Intelligent Electronic Devices (IED) are versatile computer-based devices employed in modern power systems for the purpose of protection, control and monitoring. Even though IED are usually designed to perform multiple functions, general subfunctions of an IED can be represented as shown in Figure 3.2 (based on reference [2]).

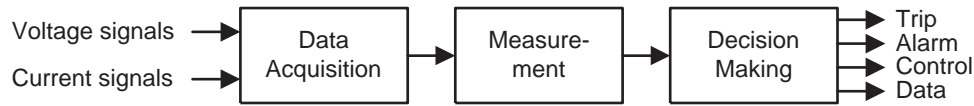


Fig. 3.2: Subfunctions of An IED

Summary of operations of the elements shown in the figure are:

- "Data Acquisition" performs front-end conditioning of the input signals. Since input signals are analog current and voltage signals, Data Acquisition filters the signals using low-pass (anti-aliasing) filter, samples the signals and digitizes the signals (by converting continuous set of input values into a discrete set). In modern IEDs, data acquisition is often built as a part of the measurement element, which is explained next.
- "Measurement" extracts desired quantities out of input signals. Typical desired quantities are current and voltage magnitude and phase, impedance, power, direction of power flow, etc. A measuring algorithm extracts the mentioned quantities. Typical techniques used to implement the measuring algorithms are Fourier transform, Differential Equation solution, etc.

- "Decision Making" derives the final output of the IED. Typical output signals are: binary (0/1) trip assertion/restrain, alarm indication, control commands, data, etc. Decision is based on a certain algorithm. The algorithm performs digital signal processing (DSP) on metered quantities, supplied by the measuring algorithm.

Flowchart of Decision Making is shown in Figure 3.3. Digital processing ranges from simple comparison of values (between measured quantities and pre-set threshold values) to sophisticated artificial intelligence methods. Results of the mentioned processing are routed to the action element. Depending on the function of an IED, action element may simply output the processed data in the desirable format (e.g. in case of power measurement) or it may issue alarm or trip signal to circuit breakers (e.g. in case of protection).

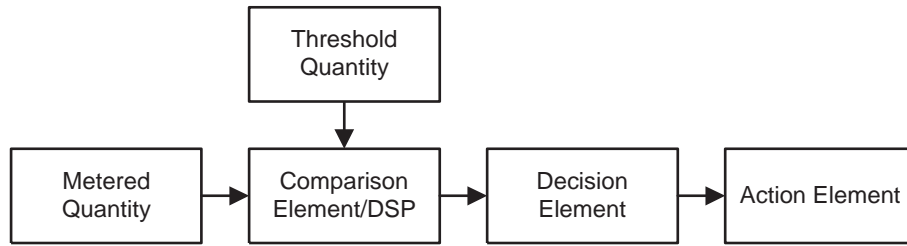


Fig. 3.3: Flowchart of Decision-Making

Evaluation of IED performance is done by evaluating performance of measuring and decision making algorithms separately. Motivation for such an approach is based on design features of modern IEDs: different IEDs performing the same function can have different measuring algorithms, while different IEDs performing different functions may rely on the same measuring algorithm. Data acquisition is not evaluated separately, because it is more efficient to regard it as a part of the measurement.

Evaluation of IED elements is done by recording available output signals, and analyzing them afterwards. Objective of the analysis is extraction of numerical values of output parameters. Definition of the mentioned parameters is given next.

3.2.3 Evaluation of a Measuring Algorithm

Measuring algorithms extract desired parameters of the input signal. Since input to the measuring algorithm are typically current and voltage signals, typical desired parameters are magnitudes and phases of sinusoidal waveforms (based on the fundamental 50Hz/60Hz frequency). The extracted values of parameters present the response of the algorithm. The response can be evaluated in two different domains: 1) time domain, 2) frequency domain. Evaluation in the mentioned domains is discussed next.

3.2.3.1 Time Responses Indices

Typical time response is shown in Figure 3.4. Performance indices are defined in Table 3.1. All the parameters of the indices are shown in Figure 3.4.

3.2.3.2 Frequency Response Indices

Evaluation of frequency response of a measuring algorithm involves notions of ideal and actual response. The responses are shown in Figure 3.5.

Ideal response Y_{ideal} is obtained using ideal band-pass filter, to extract a set of harmonics. Actual response Y_{actual} is very different from the ideal one. Difference is the presence of additional harmonic components in the actual response. Even though the amplitudes of additional components are typically suppressed significantly (in comparison with magnitudes of harmonic components that are being extracted), they have to be taken into account when evaluating frequency response of a measuring algorithm. Based on reference [10], performance indices are defined in Table 3.2.

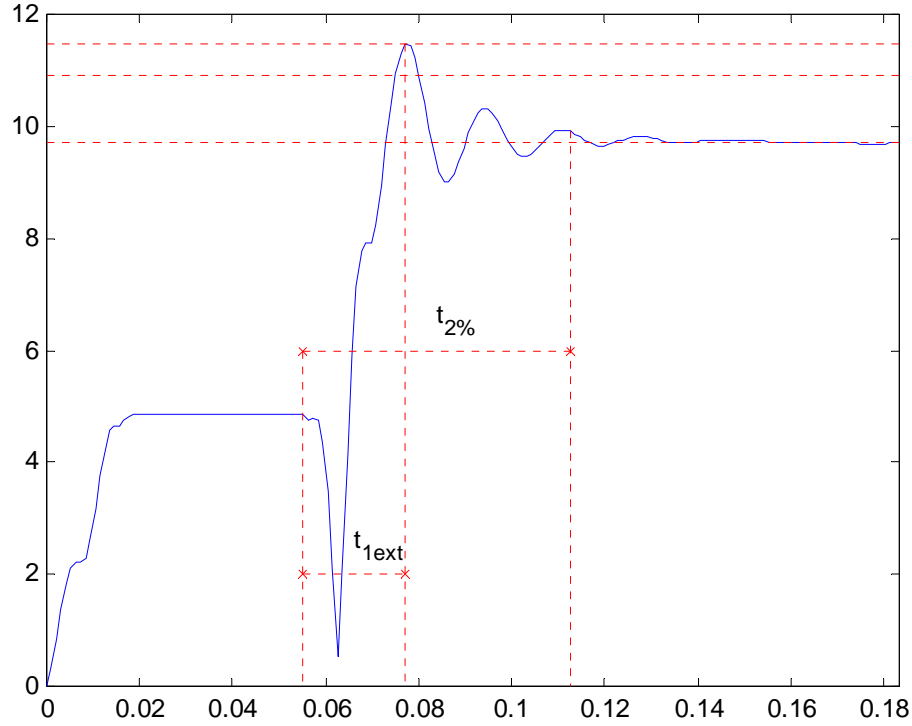


Fig. 3.4: Typical Time Response of a Measuring Algorithm

Table 3.1: Performance Indices for the Time Response of Measuring Algorithm

Index	Variable	Definition
Settling time	$t_2[s]$	Amount of time during which measured quantity transitions from the initial value to its steady-state value, with accuracy of 2 %
Time to the first maximum	$t_{1max}[s]$	Amount of time during which measured quantity reaches its first maximum value after the start of measurement
Overshoot	$\Delta y_{\%}$	$\Delta y_{\%} = \frac{y_{max} - y_{\infty}}{y_{\infty}}$
Normalized error index	e_{norm}	$e_{norm} = \frac{1}{M \cdot (y_{\infty} - y(0))} \sum_{k=L}^{L+M} (y(k) - y_a)$

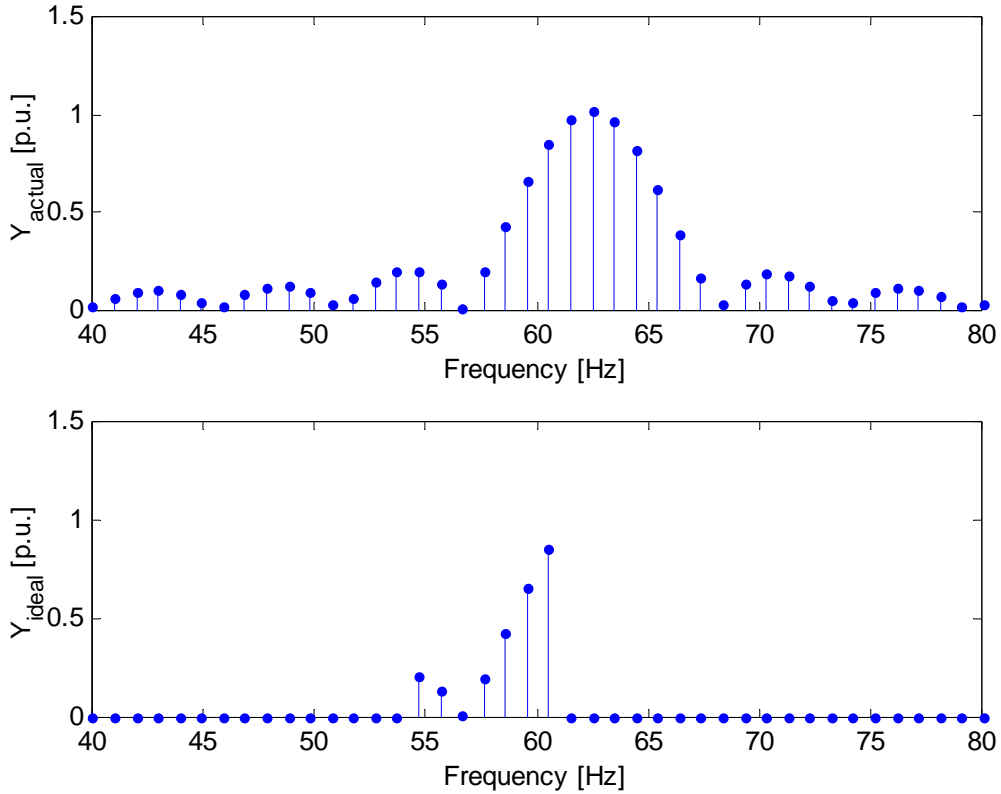


Fig. 3.5: Ideal and Actual Response of Measuring Algorithm

Table 3.2: Performance Indices for the Frequency Response of Measuring Algorithm

Index	Variable	Definition
Gain for DC component	FR_{DC}	$FR_{DC} = \frac{Y_{actual}(0)}{Y_{actual}(60)}$
Aggregated Index	F	$F = \frac{1}{f_1 - f_2} \int_{f_1}^{f_2} Y_{ideal}(f) - Y_{actual}(f) df$

3.2.4 Evaluation of a Decision-Making Algorithm

As mentioned earlier in this chapter (see Figure 3.3), objective of a decision-making algorithm is determining status of power system, based on the measurements associated with system parameters.

Changes in the power system status are associated with certain events. Event is characterized by a set of current and/or voltage waveforms, recorder (or otherwise produced) during a period of time. The period of time varies depending on IED's decision-making algorithm. Most intuitive way to evaluate performance is to evaluate how well the algorithm recognizes the power system status. Algorithm performs as expected if for a given event it recognizes a correct system state (e.g. a power quality

meter detects a certain characteristic disturbance and properly initiates necessary alarm signal). Algorithm performs unexpectedly (miss-operation), if for a specific event it makes an incorrect conclusion (e.g. a protection relay miss-interprets a minor disturbance as a fault and subsequently sends the trip command to circuit breakers). Conclusion is that decision-making criteria should reflect nature of the algorithm objective.

A starting point for development (choice) of criteria is given in reference [10]. Based on the work presented in the reference, this report defines two performance indices, to serve as the criteria. Performance indices are defined in Table 3.3. Meaning of parameters in Table 3.3 is:

- N_1 is number of events that led to correct issuance of a command signal by a decision making algorithm
- N_0 is number of events that led to correct restrain of issuing a command signal by a decision making algorithm
- N is total number of events, to which IED (decision making algorithm) was exposed (during the evaluation period).

A remark (discussion) is necessary about above-given parameters. In an ideal case, the equality $N=N_1+N_0$ holds. The physical meaning of the equality is: no events were unrecognized by decision-making algorithm. This is an ideal situation, which seldom occurs in actual field application of IEDs. Actual experience points to relation: $N>N_1+N_0$. Unrecognized events are detrimental to decision-making algorithm performance (i.e. the larger the value $N - (N_1+N_0)$, the smaller the index S , see Table 3.4)

Table 3.3: Performance Indices - Decision Making Algorithm

Index	Variable	Definition
Selectivity	S	$S = \frac{N_1 + N_0}{N}$
Average operation time	t	Amount of time between moments of event inception and decision about system status

Based on the indices defined in Table 3.3, two other indices can be defined. They are defined in Table 3.4. Mentioned indices can be derived based on definitions of dependability and security, given in reference [2]. Meaning of the parameters in Table 3.4 is:

- N_{1t} is number of events for which issuing of action signal is expected
- N_{0t} is number of events for which restrain to issuing an action signal is expected

In ideal case, the equality $N = N_{It} + N_{Ot}$ holds. Discussion, as the one given for parameters N_1 , N_0 , is valid also for parameters N_{It} , N_{Ot} . As can be seen, index S is function of both parameters s and d .

Table 3.4: Additional Performance Indices - Decision Making Algorithm

Index	Variable	Definition
Dependability	d	$d = \frac{N_1}{N_{It}}$
Security	s	$s = \frac{N_0}{N_{Ot}}$

3.2.5 Use of the Criteria

The criteria defined above is general in nature. Generality means that criteria defines framework for evaluation of any IED function. When evaluating influence of instrument transformers on a particular IED function, it is necessary to tailor the criteria. In the case of protective functions, the protection scheme may utilize several different zones of protection. To evaluate such function, it is necessary to evaluate protection in each of the zones. Examples of tailored criteria are presented in section 7. Similarly, in the case of power quality metering function, metering may involve detection of several different power quality events. To evaluate such function, it is necessary to evaluate detection of every event type. Use of criteria in project tasks can be summarized as following:

- The study addresses accuracy of optical instrument transformers. Two types of accuracies are defined in IEEE standard [11] (for more details see reference [12]):
 - Accuracy for protection purposes
 - Accuracy for metering purposes.

Both types of accuracy can be evaluated using the proposed criteria for measuring algorithm. In particular, accuracy for protection purpose may be best evaluated using time response parameters, while accuracy for metering purposes can be best evaluated using both time and frequency response parameters.

- The study addresses frequency bandwidth and dynamic range of optical instrument transformers. Frequency bandwidth can be calculated based on frequency-response of the measuring algorithm. Dynamic range can be evaluated using time-response criteria. The two mentioned features are expected to influence mostly the power quality metering function. This function can be evaluated using the criteria for decision making algorithm.
- The study addresses transient response of optical instrument transformers. Transient response can be characterized by evaluating time-response of the measuring algorithm. Transient response is expected to influence mostly protection functions. This function can be evaluated using criteria for the decision making algorithm.

3.3 Evaluation Methodology

Evaluation methodology is presented in this section. First, methodology is defined through series of answers to relevant questions. Next, possible sources of signals, for use in evaluation, are discussed. Simulation approach to evaluation is introduced afterwards. Models used in simulations are described in full detail. Process for creation of scenarios is also described. A summary is given at the end.

3.3.1 Definition of Methodology

To avoid a narrow definition, methodology is defined in the form of answers to several crucial questions. The questions and answers are:

- Why is evaluation of the influence of instrument transformers necessary and important? There are two possible reasons:
 - Conventional instrument transformers introduce signal distortions. Distortions are imposed, meaning they do not originate from the power system, rather they are introduced by instrument transformers. The source and mechanism of signal distortion within various instrument transformers designs are discussed in full detail in reference [12].
 - IEDs are sensitive to signal distortions. Consequence of this sensitivity is possible IED miss-operation. While certain miss-operations may not present critical failures (e.g. deviation in measured value by a revenue meter), there are miss-operations that have been shown to lead to disastrous situations (e.g cascading, incorrect opening of healthy transmission lines by protective relays). The full aspects of the mentioned sensitivity are not discussed in detail in this report. Exhaustive coverage of some aspects of the topic can be found in references [13], [14], [15], [16].
- How can the influence of instrument transformers be measured? The influence can be measured using performance indices, previously defined this section. The indices can be used as the criteria in a context of an IED function. In this case, instrument transformer performance is not evaluated directly; rather performance of IED function is evaluated. By comparing performance of the same function in two distinct situations, influence of a particular instrument transformer on the function can be evaluated. The two situations are:
 - IED is exposed to signals supplied by a referent instrument transformer
 - IED is exposed to signals supplied by specific (actual) instrument transformer

Difference in the mentioned situation may seem subtle and irrelevant at first glance. However, it is very distinct and crucially significant. Difference in terms "referent" and "specific", when referencing instrument transformers, reflects the logic behind the evaluation methodology. Term "specific" denotes an instrument transformer that is intended to be evaluated (e.g. newly-acquired current transformer, that is about to be commissioned into service). Term "referent" denotes an instrument transformer that has the following two characteristics:

- Known performance, meaning that instrument transformer has been evaluated for its accuracy through either field application or laboratory testing
- Stable performance, meaning that performance has not deteriorated over a long period of time

The intention behind referent instrument transformer is to establish an approximation of an ideal instrument transformer.

- *What are the means for quantifying the influence (obtaining numerical values)?* Numerical values of indices defined in this section can be used for quantifying the influence. Specific formulas for calculation of indices are given in Tables 3, 4, 5.
- *What is the best procedure for finding the quantitative values of the influence?* The best procedure is a statistical analysis of recorded output signals from IEDs. Term "statistical" means that a sufficiently large number of signals should be available for analysis (number depending on the type of function performed by IED). Term "analysis" means extraction (calculation) of numerical values of criteria from IED output signals.

Based on the mentioned question and answers, methodology can be summarized as a following procedure:

1. Expose IEDs to sufficient number of power system events
2. Record IED output signal(s) during exposure to events
3. Analyze recorded signals in order to extract numerical values of performance indices
4. Repeat steps 1 through 3 using a referent and a specific instrument transformer
5. Compare numerical values of indices

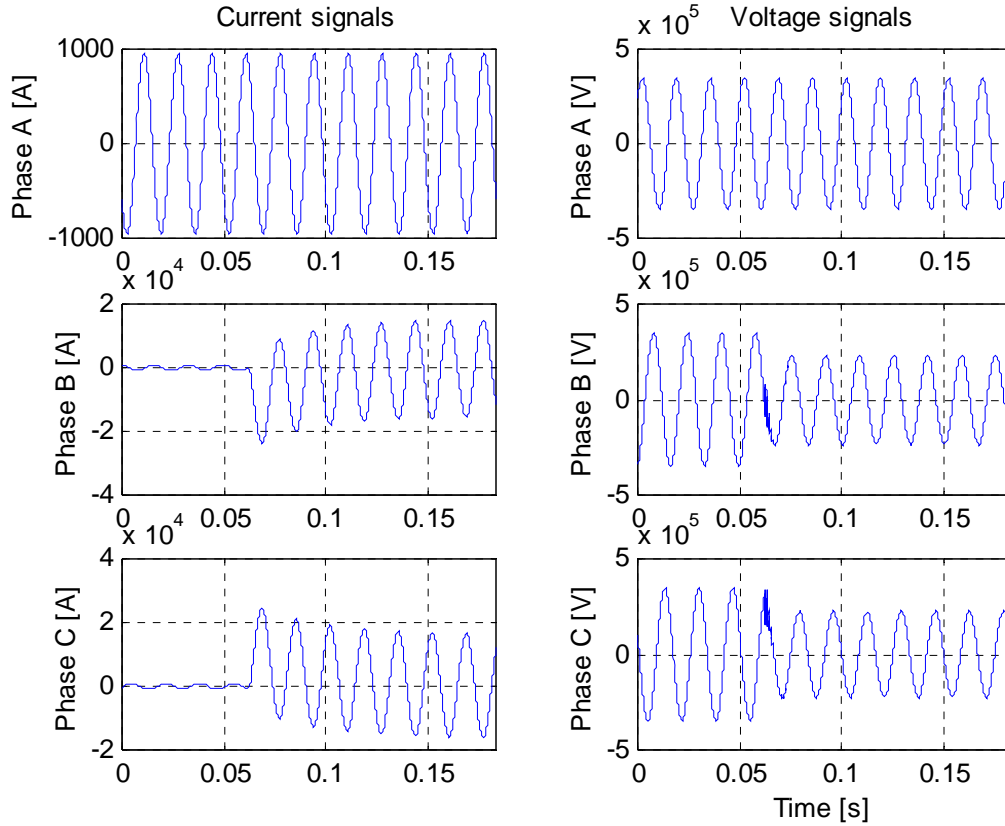


Fig. 3.6: Exposure signals from a fault event

3.3.2 Exposure Signals

In the definition of evaluation methodology, statistical analysis was chosen as the most appropriate procedure for calculation of numerical values of performance indices. Statistical analysis is based on output signals from IEDs. Output signals are initiated by certain input signals, called exposures. Input signals from a given power system event constitute a single exposure. There are several definitions of a power system event (see references [17], [10], [18]). Definition of an event depends primarily on the type of function that responds to the event. In this report, event is defined as:

- Disturbance that triggers power quality meter to issue assertive output signal
- Disturbance or fault that triggers protective relay to issue either assertive (trip-permitting) or restraining (blocking) output signal

An example of exposure signals (waveforms) associated with a phase-to-phase (B-to-C) fault on a transmission line is shown in Figure 3.6.

For statistical analysis, typically a large number of events are necessary in order to evaluate IED behavior. There are two sources of exposure signals:

- Field-recorded data

- Data obtained from simulations

Exposures Recorded in the Field

There were two sources of field-recorded data available through this project:

1. ION84000 meter. This IED records the following data (see reference [19])
 - True RMS 3-phase voltage, current and power
 - Instantaneous 3-phase voltage, current, frequency, power factor
 - Bi-directional, absolute, net, time-of-use, loss compensation energy
 - Rolling block, predicted, thermal demand
 - Individual, total harmonic distortion up to the 63rd harmonic
 - Sag/Swell
 - Number of Nines (power availability)
 - Symmetrical components
 - K-Factor for voltage and current inputs
2. TESLA recorder. This IED is a digital fault recorder. It captures current and voltage signals for a period of time, when triggered by a certain event. Recorded data can be accessed through remote, dial-up connection, using TESLA access software.

Exposures Created By Simulation

Data mentioned in the previous subsection can be produced through simulation. One advantage of data created by simulation is that a large number of different events can be simulated. This number is usually much larger than the number of disturbance and faults that can be captured in the field. Purpose of data created by simulation is:

- Validation of instrument transformer models
- Validation of IED models
- Validation of power network model
- Evaluation of instrument transformer models

3.3.3 Evaluation Based on Simulation

Objective of simulation is to examine behavior of models of instrument transformers and IEDs. By simulating various power system events, influence of instrument transformer models on IED model behavior can be evaluated. The steps for simulation approach are:

1. Create a database of exposure signals. Events are simulated according to selected scenarios. Simulations incorporate power network and instrument transformer models. Output signals from simulations are taken from the secondary connections of instrument transformers. Output signals are stored (recorded) as files. Typically, number of exposure event files is very large, and constitutes a database of events. Every exposure file is independently accessible for later analysis.
2. Subject IED models to exposure signals. Exposure means replaying current and voltage signals at the input of IED models. Replaying creates the same conditions on the input of IED model as if the model was connected directly to instrument transformer secondary output during a particular event.
3. Create a database of IED model responses. During exposure, IED produces certain output signal(s). Output signals are recorded as separate files. Number of response files is equal to number of exposures. Every response file is independently accessible for later analysis.

The above-mentioned steps are shown in Figure 3.7. Shaded elements represent points in simulation procedure where output is recorded (stored in a file). Once the IED model responses are recorded, they can be used for calculation of performance indices.

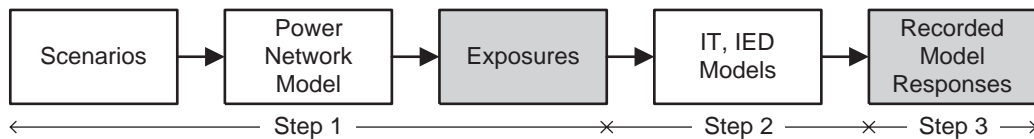


Fig. 3.7: Steps of the Simulation Approach

3.3.4 Models Used in Simulations

There are three types of models used in simulations:

1. Power network.
2. Instrument transformers
3. IEDs

3.3.4.1 Power Network

Model of power network should reflect the following characteristic of realistic systems:

- Impedance characteristics of transmission lines
- Dynamic characteristics of pertinent equipment (e.g. generators, transformers, etc.)
- Interconnections with other portions of the power system grid

The above-given list is not exhaustive; however, it does cover the most critical items. Impedance characteristics include non-linear behaviors and frequency dependencies. Portions of power system grid, interconnected with section under consideration, should be presented by their Thevenin's equivalents. Power network model used in this report is shown in Figure 3.8. Model was derived from physical measurements on the Sky-STP section of CenterPoint Energy grid. The section is 9-bus, 11-lines, 345 kV power grid. More details about the network model (characteristics, behavior) can be found in reference [20].

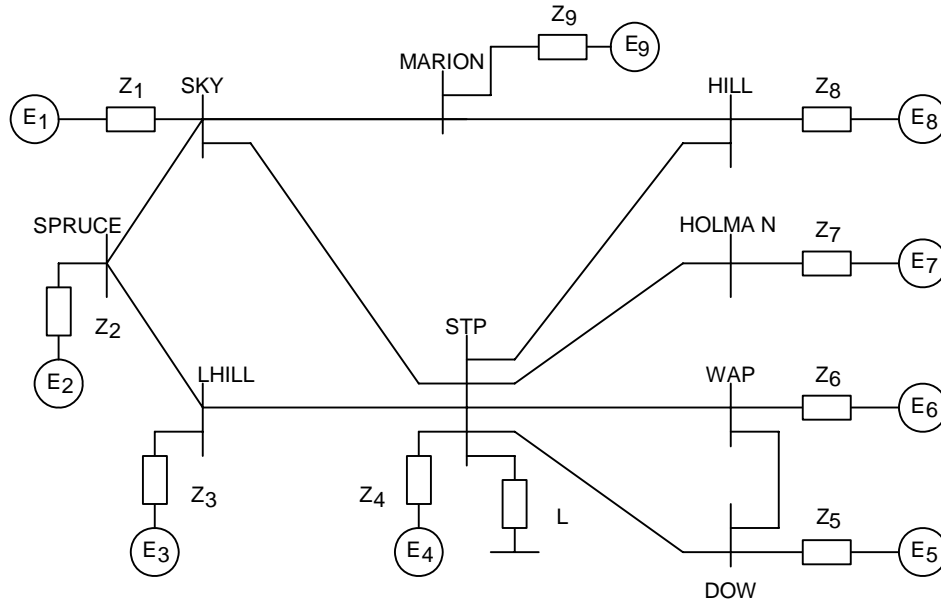


Fig. 3.8: Model of Power Network

3.3.4.2 Current Transformer

A total of four current transformer models were used in simulations. The models are based on an equivalent circuit shown in Figure 3.9. Parameters of circuit are shown in Table 3.5. More details about the equivalent circuit can be found in reference [21].

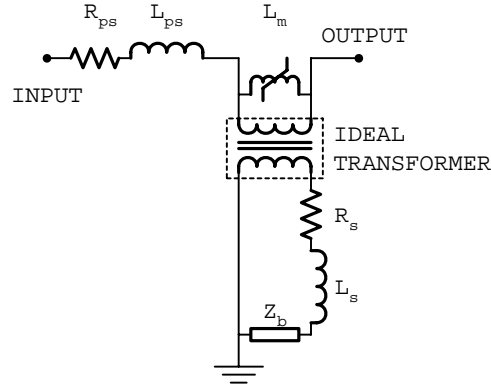


Fig. 3.9: Equivalent Circuit of Current Transformer Model

Table 3.5: Parameters of Equivalent Circuit of Current Transformer Model

Parameter	Value
Turns ratio	900:5
Mean core length	0.4987 m
Cross-section area	$1.91532 \times 10^{-3} \text{ m}^2$
Winding resistance	0.253 ohms
Remnant flux	0.4645 V
R_{ps}, L_{ps}	~ 0
R_s	0.33 ohms
L_s	~ 0
L_m	defined by V-I characteristic

In the report on Task \#1 it was pointed out that the most problematic aspect of the influence of current transformers is the transient response. Distortions in transient response are caused primarily by saturation (see section 2.5.1. in reference [12]). Parameters of a current transformer model that influence saturation are:

- V-I characteristic of the electromagnetic core
- Transformer burden

Two different V-I characteristics, and two different burdens were modeled, giving total of four different current transformer models. V-I characteristics are shown in Figure 3.10. The burdens are: $Z_{B1}=1.33+j0.175$ ohms, $Z_{B2}=8.33+j0.175$ ohms. The magnitudes of burdens, 1.34 ohms and 8.33 ohms respectively, are equivalent to magnitudes of standard burdens B-1 and B-8 (definitions can be found in IEEE standard, reference [11]). Parameters of models are summarized in Table 3.6.

Table 3.6: Parameters of Current Transformer Models

Model	V-I characteristic	Burden
1	1	Z_{B1}
2	1	Z_{B2}
3	2	Z_{B1}
4	2	Z_{B2}

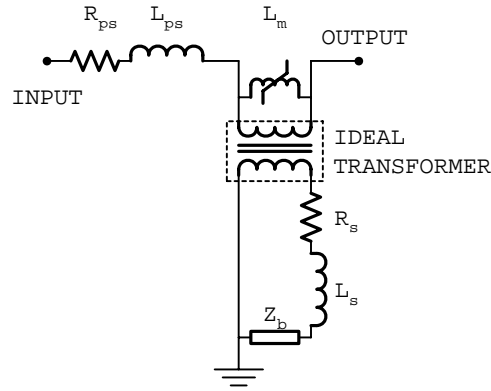


Fig. 3.10: V-I Characteristics of Electromagnetic Core of a Current Transformer

3.3.4.3 Coupling-Capacitor Voltage Transformer

Frequency bandwidth and transient response were identified as the most problematic aspects of CCVT influence in [12] (see sections 2.4.2. and 2.5.2). Frequency bandwidth is limited by stray capacitances, while transient response is distorted by voltage-subsidence and ferroresonance effects. Mentioned distortions originate in:

- Configuration of the transformer components
- Transformer burden

Two different configurations, and two different burdens were implemented, thus giving a total of four different models. Configuration is shown in Figure 3.11. The burdens are: $Z_{B1}=100$ ohms, $Z_{B2}=j100$ ohms. Parameters of models are summarized in Table 3.7.

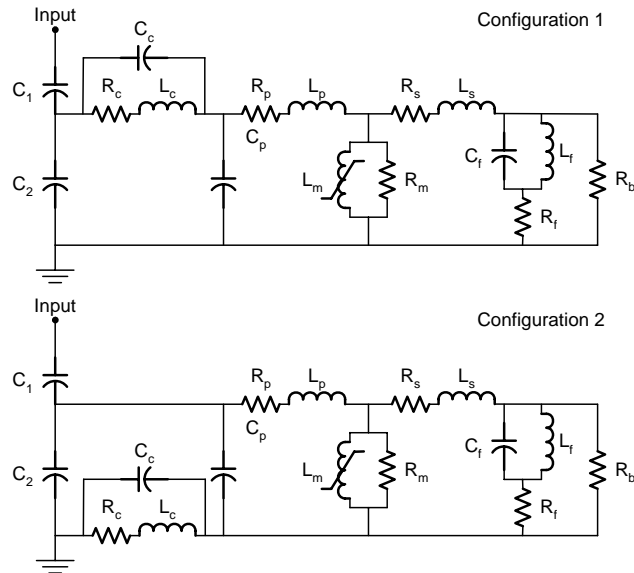


Fig. 3.11: Configurations of Coupling-Capacitor Voltage Transformers

Table 3.7: Parameters of Coupling-Capacitor Voltage Transformer Models

Model	Configuration	Burden
1	1	Z_{B1}
2	1	Z_{B2}
3	2	Z_{B1}
4	2	Z_{B2}

3.3.4.4 Overcurrent Protection Numerical Relay (Model A)

Three models of IEDs, denoted A,B,C, are modeled for the purpose of this project. The correspondence between models and actual equipment used in AEP Corridor installation is summarized in Table 3.8. Remark: GE F60 is not installed in AEP field. However, since model D60 was unavailable at times, during derivation of results for this report, F60 was modeled for some test results.

Table 3.8: IED and Models

IED	Model
SEL-321	B
GE D60	B
GE F60	A
ION8400	C

The overcurrent relay model is denoted as IED model A. Features of the model are:

- Three-phase directional instantaneous overcurrent protection as primary protection
- Three-phase time overcurrent protection as backup protection
- Residual time overcurrent protection

Functional elements of the model and their functions are:

- Measuring element extracts current and voltage phasors from the input signals. Extraction is performed based on Fourier analysis of input signals. Four signals: 1) current magnitude, 2) current phase, 3) voltage magnitude, 4) voltage phase, are multiplexed together, and produced as a single signal at the output of the measuring element.
- Overcurrent element consists of 3 sub-elements. Each of the sub-elements implements a certain protection principle. Output signals of the sub-elements are produced independently at the output of the overcurrent element. The sub-elements and their functions are:
 - Time overcurrent protection uses inverse-time characteristic to determine time-to-operate (period of time between detection of over-the-threshold current magnitude and assertion of trip command). Time-inverse characteristic

allows for fast operation in case of high-level fault currents, and for slow operation in case of low-level fault currents.

- Residual time overcurrent protection offers the same kind of protection as the time overcurrent protection, except the residual sub-element is active only when a fault involving ground is detected.
- Directional protection determines direction of the flow of the power to determine whether a potential fault is in the direction of protected zone. It does not directly produce trip command; rather, it restrains assertion of trip command in case of faults in direction opposite to protected zone.
- Logic element performs certain logic functions (AND, OR) to derive trip asserting or trip blocking command at the output of the relay model. The logic is implemented to improve security and dependability of the model.

3.3.4.5 Line Impedance Protection Numerical Relay (Model B)

Line distance relay model is denoted as IED model B. Features of the model are:

- Three separate MHO forward sensing zones for multi-phase faults
- Three separate "quadrilateral" forward sensing zones for phase to ground faults
- One MHO reverse sensing zone for multi-phase faults
- One "quadrilateral" reverse sensing zone for phase to ground faults
- Six separate MHO starters, one for each fault-measured loop
- Undervoltage element

Functional elements of the model and their functions are:

- Measuring algorithm extracts impedance using differential algorithm. Impedance is extracted from the input current and voltage signals. Impedance (distance) to fault is calculated using expressions for six basic fault types: AG, BG, CG, ABC, BC, CA (letter G denotes ground). Impedances to fault (apparent impedances) for every of the six fault types are multiplexed and sent as a single signal to the next element.
- Fault identification element determines whether calculated impedance falls into reach of any of the user-preset zones. The check is performed for every of the zones and every of the six basic fault types. Resulting binary signals (1/0, denoting impedance inside/outside of the zone, respectively) are multiplexed and sent as a single signal to the next element.

- Fault classification element determines fault type, based on impedance calculated for six basic fault types. The output of this element is not necessary for determination of command signal of relay model (trip assertion or blocking signal). However, output of this element is very useful information for protection engineers.
- Logic element performs certain logic functions (AND, OR) to derive trip asserting or trip blocking command at the output of the relay model (similarly as in the case of IED model A).

3.3.4.6 Power Quality Meter (Model C)

Power quality meter model is denoted as IED model C. Features of the model are:

- Detection of disturbances
- Classification of disturbances as power quality events

Functional elements of the model and their functions are:

- Feature extraction element captures distinct, dominant patterns in the metered signals. The capturing of patterns is done using Fourier and wavelet transforms. Patterns characterize typical power quality events.
- Detection and classification element decides on the event type, based on its features. There are six event types that can be recognized:
 1. Flicker
 2. Impulse
 3. Swell
 4. Sag
 5. Transient
 6. Harmonic

3.4 Conclusion

Evaluation methodology is presented in this section. Methodology is defined as a procedure. Procedure is based on series of relevant questions and answers. Conclusion is that methodology can be best implemented through simulation. By defining simulation models and scenarios, it was shown that simulation can produce all evaluation results.

4. Assessment of the Benefit of Higher Accuracy

4.1 Introduction

Accuracy for protection purposes can be best evaluated using time response parameters, this is done using IED models A and B and results are presented later in this report. Accuracy for metering purposes can be evaluated using time response (related to dynamic range) and frequency response (frequency bandwidth) parameters. Then, IED model C (power quality meter) will be used to generate scenarios for analysis.

4.2 Scenarios

Power quality meter model is denoted as IED model C. Features of the model are:

- Detection of disturbances
- Classification of disturbances as power quality events

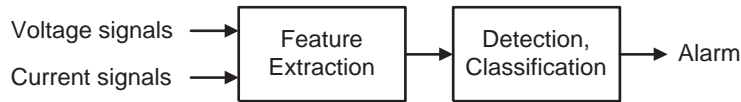


Fig. 4.1: Functional Elements and Flowchart of IED Model C

Functional elements and flowchart of the model are shown in Figure 4.1. Elements and their functions are:

- Feature extraction element captures distinct, dominant patterns in the metered signals. The capturing of patterns is done mostly by using Fourier or wavelet transforms. Patterns characterize typical power quality events.
- Detection and classification element decides on the event type, based on its features. There are three event types that will be recognized:
 - Flicker
 - Swell
 - Sag

Events are created differently depending on the type of disturbance to be simulated. Tables 4.1 – 4.2 summarize scenario definitions for all simulated disturbances:

Table 4.1: Simulation Scenario, IED Model C, Voltage Sag/Swell

Feature	Parameters
Type	Three phase - Single phase - Phase to Phase - Two phase to ground
Phase Angle Shift [deg]	0, -30, -60
Duration [cycles]	3, 6, 9
Magnitude [pu]	0.3, 0.6, 0.9

Table 4.2: Simulation Scenario, IED Model C, Flicker

Feature	Parameters
Modulation Component Frequency [Hz]	5, 10, 20, 5 - 10, 5 -20, 10 - 20
Modulation Component Magnitude [pu]	0, -30, -60

4.3 Evaluation Results

The main function of a power quality meter is to detect, classify and characterize power quality disturbances, i.e. to define and obtain distinctive and pertinent parameters to describe specific types of disturbance waveforms [22]. Performance indices of a power quality meter should provide an estimate of its ability to properly detect and characterize different kinds of power quality events. Based on the ability of the power quality meter to correctly detect a disturbance the following index can be defined:

The performance index of power quality meter P when fed by exposure E is denoted by $PQPI_P^E$. The average performance index of power quality meter P is defined as:

$$PQPI_P = \frac{1}{N} \sum_{E \in EDB} PQPI_P^E$$

There are two types of calculations for the power quality performance index; these are the detection method and the characterization method. For the detection method:

$$PQPI_P^E = |D^t - D^r|$$

Where:

$$D^t, D^r = \begin{cases} 1 & \text{if } PQ \text{ meter properly detects disturbance} \\ 0 & \text{otherwise} \end{cases}$$

For the characterization method:

$$PQPI_P^E = |D^t - D^r|$$

Where D^t, D^r stand for the estimated value for the characterization feature (i.e. phase angle shift, duration, magnitude, modulation RMS, etc) of the tested and the referent power quality monitoring system.

Results of evaluation of the accuracy of conventional and non-conventional instrument transformers are presented in this section. Results are obtained using simulation. Again, evaluation results are presented in the form of performance indices.

Table 4.3: Sag and Swell Characterization

Model	Detection Method	Sag/Swell Characterization	
	PQPI - Detection	PQPI - Duration	PQPI - Average RMS
Sag	0	0.002	0.021
Swell	0	0	0.022

Table 4.4: Flicker Characterization

Model	Detection Method	Flicker Characterization	
	PQPI - Detection	PQPI - Peak Value	PQPI - Modulation RMS
Flicker	0	0.007	0.001

4.4 Assessment of Higher Accuracy

Performance of the sag/swell detection and characterization algorithm

The following conclusion can be made based on the results:

- There is no influence on the PQ meter's ability to properly detect power quality disturbances such as voltage sags/swells.
- Influence on calculation of sag/swell's duration and signal's average RMS value is negligible.

Performance of the flicker detection and characterization algorithm

The following conclusion can be made based on the results:

- There is no influence on the PQ meter's ability to properly detect voltage flickering.
- Influence on calculation of peak value of the signal and modulation RMS is negligible.

4.5 Conclusion

Results of evaluation of accuracy of conventional and non-conventional instrument transformers are presented in this section. Practical, numerical values have been illustrated. It was shown that conventional instruments would not influence the ability of the power quality meter to properly detect and characterize power quality events such as voltage sags, swell and flickering.

5. Assessment of the Benefit of Wider Frequency Bandwidth

5.1 Introduction

This section addresses frequency bandwidth of optical instrument transformers. This feature is expected to influence power quality metering functions. Results that evaluate impact of frequency bandwidth on power quality metering functions are also presented in this section of the report.

5.2 Evaluation of Frequency Bandwidth

Accuracy for metering purposes can be evaluated using time response (related to dynamic range) and frequency response (frequency bandwidth) parameters. Evaluation of accuracy has been presented at the end of section 4 of this report. Even though a model of the optical voltage transformer was not available for the use in simulations, evaluation of the impact of a CCVT limited frequency bandwidth on the performance of a PQ meter algorithm has been studied. The IED model C (power quality meter) will be used to generate scenarios for the analysis.

5.2.1 Scenarios

Power quality meter model is denoted as IED model C. Features of the model are:

- Detection of disturbances
- Classification of disturbances as power quality events



Fig. 5.1: Functional Elements and Flowchart of IED Model C

Functional elements and flowchart of the model are shown in Figure 5.1. Elements and their functions are:

- Feature extraction element captures distinct, dominant patterns in the metered signals. The capturing of patterns is done using Fourier and wavelet transforms. Patterns characterize typical power quality events.
- Detection and classification element decides on the event type, based on its features. There are two event types that will be recognized:
 - Harmonics
 - Transients

Events are created differently depending on the type of disturbance to be simulated. Tables 5.1 – 5.2 summarize scenario definitions for all simulated disturbances:

Table 5.1: Simulation Scenario, IED Model C, Harmonics

Feature	Parameters
Harmonic Order	h=3, 5, 7, 9
Harmonic Magnitude [pu]	0.06, 0.1, 0.2

Table 5.2: Simulation Scenario, IED Model C, Transients

Feature	Parameters
Point on wave [deg]	0, 45, 90, 135, 180
Oscillatory Component Magnitude [pu]	0.5, 1, 1.5
Oscillatory Component Frequency [Hz]	300, 600, 1200, 2400

5.2.2 Evaluation Results

Results of evaluation of the frequency bandwidth of conventional instrument transformers are presented in this section. Results are obtained using simulation. Again, evaluation results are presented in the form of performance indices.

Table 5.3: Harmonics Characterization

Model	Detection Method	Harmonics Characterization		
	PQPI - Detection	PQPI - Average RMS	PQPI - THD	PQPI - Harmonic Magnitude
Harmonics	0.083	0.009	0.027	0.026

Table 5.4: Transients Characterization

Model	Detection Method	Transients Characterization	
	PQPI - Detection	PQPI - Peak Value	PQPI - Duration
Transients	0.104	0.429	0.026

5.3 Assessment of Wider Frequency Bandwidth

Performance of the harmonic detection and characterization algorithm

The following conclusion can be made based on the results:

- Influence on PQ meter's ability to properly detect harmonics is negligible for low order harmonics. Higher order harmonics were not considered since CCVTs do not provide accurate representation of higher-frequency components.
- Influence on calculation of signal's average RMS value is negligible.

- Considering an average tested THD of 0.12 pu, the PQPI – THD shows a considerable difference in the ability of the algorithm to properly characterize THD (22.5 percent difference), even for low order harmonics.

Performance of the voltage transient detection and characterization algorithm

The following conclusion can be made based on the results:

- Influence on the PQ meter's ability to properly detect voltage transients is considerable (from PQPI – Detection we see that in more than 10 percent of the cases detection was not achieved). This is especially true for transients with high frequency oscillatory components.
- Influence on calculation of transient's peak value is also considerable. Even if the transient could be detected when exposing the algorithm to signals coming from conventional ITs, there is a percent difference of 18.2 percent when compared to the referent system (PQPI of 0.429 for an average 2.36 peak value)
- Influence on calculation of transient's duration is very substantial. For an average simulated transient duration of 0.018 sec the calculated PQPI is 0.026 sec, which is equivalent to a percent difference of 144 percent.

5.4 Conclusion

Results of evaluation of frequency bandwidth of conventional and non-conventional instrument transformers are presented in this section. It was shown how the choice of criteria can be used for assessment of the influence of the limited frequency bandwidth of conventional voltage transformers on power quality events detection and/or characterization. Practical, numerical values have been illustrated. Conclusion is that simulation environment can be used to obtain results for task #5.

6. Assessment of the Benefit of Improved Transient Response

6.1 Introduction

This section addresses transient response of optical instrument transformers. The transient response is expected to influence protection functions. Results that evaluate accuracy for protection purposes are also presented in this section.

6.2 Evaluation of Transient Response

6.2.1 Scenarios

Events are created according to the simulation scenarios. Scenario is a description of power system behavior. Definitions of a scenario consist of:

- Timeline of events
- Features of events

Meaning of a scenario is:

- Timeline of events defines the moments when a certain change occurs in the power system model. Change is usually approximated by a switching sequence. Switching allows for alternations in the topology of the network model , thus simulating faults and disturbances.
- Features of events characterize the nature of an event. Examples of features are: location of a fault along the transmission line, associated resistances (such as grounding or line-to-line resistances), point-on-wave of fault inception and so on.

Different scenarios were created for evaluation of the transient response of IED models A and B. Three fault types were simulated: AG, BC, ABCG. Simulated fault types cover phase-to-ground (AG) faults, phase-to-phase (BC) faults, as well as three-phase-to-ground (ABCG). IEDs that are modeled should not be sensitive to a change in fault type (considering selectivity and operation time). Every fault type was simulated at four locations, along the protected Sky-STP line. The locations are:

- IED model A: -10, 10, 70 and 90 percent of the line length
- IED model B: 70, 75, 85 and 90 percent of the line length

Location -10 percent (in case of IED model A) denotes fault simulated in backward direction i.e. at 10 percent of the Sky-Spruce line length. Fault locations of 70 and 75 percent should be detected by IED model B in its first zone. Locations of 85 and 90 percent should be detected in its second zone. In relaying terms, locations of 75 and 85 percent are very close to the point between the zones (80 percent of line length). By

simulating faults at two mentioned locations, it can be checked whether IED model B is overreaching or underreaching.

Every fault is simulated using two fault resistances: $0\ \Omega$ and $5\ \Omega$. In case of phase-to-ground faults, the mentioned resistances are used for grounding, while in case of phase-to-phase faults; the resistance is used as connection between the phases. Finally, every fault was simulated using eight different fault inception points-on-wave, covering range of one 60 Hz cycle in eight equal, consecutive time-steps.

Scenario definitions are summarized in Tables 6.1 and 6.2.

Table 6.1: Simulation Scenario, IED Model A

Feature	Parameters
Fault type	AG, BC, ABCG
Fault Location [%]	-10, 10, 70, 90
Resistance [Ω]	0, 5
Point-on-wave [deg]	0, 45, 90, 135, 180, 225, 270, 315

Table 6.2: Simulation Scenario, IED Model B

Feature	Parameters
Fault type	AG, BC, ABCG
Fault Location [%]	70, 75, 85, 90
Resistance [Ω]	0, 5
Point-on-wave [deg]	0, 45, 90, 135, 180, 225, 270, 315

6.2.2 Evaluation Results

Results of evaluation of the transient response of conventional instrument transformers are presented in this section. Results are obtained using simulation environment. Influence of instrument transformer models on IED models A and B is evaluated. Functional elements of IED models were tested separately. The evaluation results are in the form of numerical values of performance indices.

Measuring algorithm is evaluated using performance indices defined in section 5.2. Decision-making algorithm is evaluated using performance indices tailored to functions performed by IED models. In evaluation of the model A, meaning of criteria parameters is:

- N_1 is number of correct trip assertions for faults in forward direction
- N_2 is number of correct trip restrains for faults in backward direction
- F_1 is number of incorrect trip restrains for faults in forward direction
- F_2 is number of incorrect trip assertions for faults in backward direction
- s_I is defined as:

$$s_1 = \frac{N_1}{N_{forward}}$$

- s_2 is defined as:

$$s_2 = \frac{N_2}{N_{backward}}$$

Where $N_{forward} = 48$ is number of faults simulated in the forward zone of protection, and $N_{backward} = 16$ is number of faults simulated in the backward zone. Ideal IED performance would produce $N_1 = 48$ and $N_2 = 16$. In the case of IED model B, meaning of criteria parameters is:

- N_1 is number of correct trip assertions for faults in primary zone of protection
- N_2 is number of correct trip assertions for faults in backup zone of protection
- F_1 is number of trip assertions with incorrect time-delay, for faults in primary zone of protection (faults detected as belonging to the backup zone)
- F_2 is number of trip assertions with incorrect time-delay, for faults in backup zone of protection (faults detected as belonging to the primary zone)
- s_1 is defined as:

$$s_1 = \frac{N_1}{N_{primary}}$$

- s_2 is defined as:

$$s_2 = \frac{N_2}{N_{backup}}$$

where $N_{primary} = 32$ is number of faults simulated in primary zone of protection, and $N_{backup} = 32$ is number of faults simulated in backup zone. Ideal IED performance would produce $N_1 = 32$ and $N_2 = 32$. Indices t_1 and t_2 are average tripping times for faults in primary and backup zones, respectively (average tripping time is calculated only for correct trip assertions). An example of input signals is shown in Figure 6.1. Waveforms in the Figure depict ABC-phase-to-ground fault.

6.2.2.1 IED Model A

Output signals from both the measuring element and decision making element are available for IED model A. First, results of evaluation of measuring elements are presented. Next, results of evaluation of decision-making element are given. All the results are discussed. Relevant conclusions are summarized.

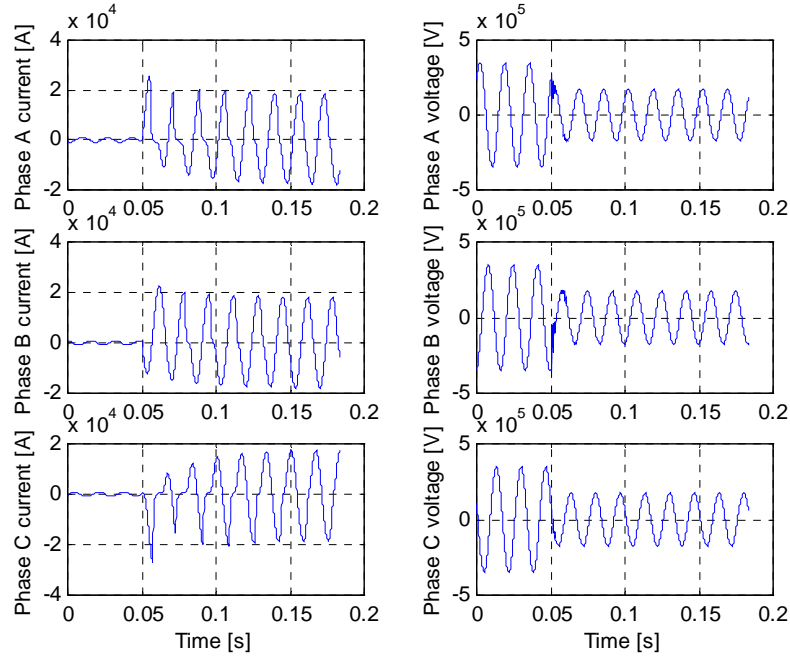


Fig. 6.1: Signals associated with abc-phase-to-ground fault

Performance of the current measuring algorithm

The most problematic aspect of the influence of current transformers is the transient response. Distortions in the transient response are caused primarily by saturation (see section 2.5.1. in reference [12]). Performance indices that can be used for detection of saturation are:

- Time to the first maximum, t_{1max}
- Overshoot, $\Delta y_{\%}$

In the case the saturation occurs in large number of test cases:

- Settling time is expected to increase, when compared to performance of referent instrument transformer
- Overshoot is expected to decrease, when compared to performance of referent instrument transformer

The above-mentioned situations are illustrated in Figure 6.2. Evaluation results for the current measuring element are given in Tables 6.3 through 6.5.

Table 6.3: Current Measuring Element, ABCG Fault

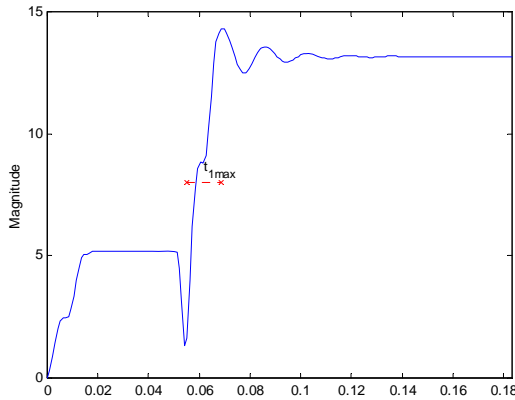
Model	$t_{2\%}$	$\Delta y_{\%}$	$\Delta e_{\%}$	FR_{DC}	F
Referent	0.126	0.082	0.019	0.283	0.004
CT 1	0.126	0.079	0.070	0.175	0.005
CT 2	0.126	0.015	0.551	0.036	0.006
CT 3	0.126	0.100	0.054	0.215	0.005
CT 4	0.126	0.047	0.164	0.073	0.005
OCT 1	0.126	0.091	0.036	0.236	0.004
OCT 2	0.126	0.091	0.038	0.236	0.004

Table 6.4: Current Measuring Element, AG Fault

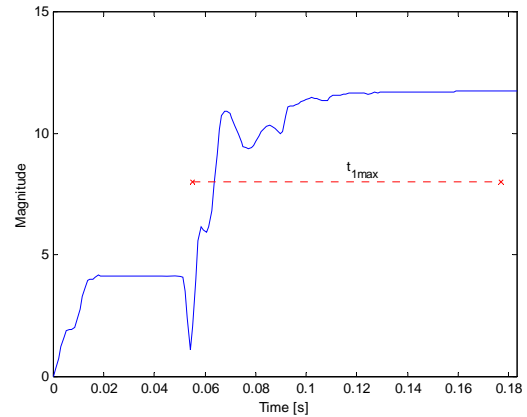
Model	$t_{2\%}$	$\Delta y_{\%}$	$\Delta e_{\%}$	FR_{DC}	F
Referent	0.126	0.041	0.026	0.053	0.003
CT 1	0.126	0.044	0.100	0.038	0.003
CT 2	0.107	0.024	0.318	0.022	0.003
CT 3	0.126	0.045	0.052	0.041	0.003
CT 4	0.117	0.039	0.168	0.030	0.003
OCT 1	0.126	0.042	0.043	0.053	0.003
OCT 2	0.126	0.042	0.045	0.053	0.003

Table 6.5: Current Measuring Element, BC Fault

Model	$t_{2\%}$	$\Delta y_{\%}$	$\Delta e_{\%}$	FR_{DC}	F
Referent	0.126	0.056	0.052	0.193	0.004
CT 1	0.126	0.055	0.115	0.127	0.004
CT 2	0.126	0.010	0.452	0.020	0.005
CT 3	0.126	0.070	0.085	0.150	0.004
CT 4	0.126	0.044	0.184	0.059	0.004
OCT 1	0.126	0.056	0.068	0.193	0.004
OCT 2	0.126	0.056	0.070	0.193	0.004



a) Original Waveform



b) Distorted Waveform

Fig. 6.2: Comparison of Performance Index t_{1max} .

Performance of the voltage measuring element algorithm

Evaluation results for the voltage measuring element are given in Tables 6.6 through 6.8. In this case, only models of traditional voltage transducers have been used since as it was previously stated, a model of the optical voltage transducer was not available.

Table 6.6: Voltage Measuring Element, ABCG Fault

Model	$t_{2\%}$	$\Delta y_{\%}$	$\Delta e_{\%}$	FR_{DC}	F
Referent	0.126	0.029	-0.004	0.022	0.003
CCVT 1	0.126	0.043	0.000	0.018	0.002
CCVT 2	0.126	0.140	-0.001	0.018	0.003
CCVT 3	0.126	0.048	0.000	0.018	0.002
CCVT 4	0.126	0.179	-0.006	0.019	0.003

Table 6.7: Voltage Measuring Element, AG Fault

Model	$t_{2\%}$	$\Delta y_{\%}$	$\Delta e_{\%}$	FR_{DC}	F
Referent	0.065	0.009	-0.035	0.011	0.001
CCVT 1	0.065	0.011	-0.030	0.011	0.001
CCVT 2	0.065	0.025	-0.030	0.011	0.001
CCVT 3	0.065	0.010	-0.030	0.011	0.001
CCVT 4	0.065	0.029	-0.031	0.011	0.001

Table 6.8: Voltage Measuring Element, BC Fault

Model	$t_{2\%}$	$\Delta y_{\%}$	$\Delta e_{\%}$	FR_{DC}	F
Referent	0.065	0.017	-0.153	0.010	0.001
CCVT 1	0.065	0.013	-0.150	0.008	0.001
CCVT 2	0.065	0.026	-0.150	0.008	0.001
CCVT 3	0.065	0.016	-0.150	0.008	0.001
CCVT 4	0.065	0.031	-0.150	0.008	0.001

Performance of the decision-making algorithm

Evaluation results for the decision-making element are given in Tables 6.9 through 6.11.

Table 6.9: Overcurrent Decision Element, ABCG Fault

Model	N_1	F_1	N_2	F_2	s_1	s_2	$t[s]$
Referent	48	0	16	0	1	1	0.021
CT 1	48	0	16	0	1	1	0.025
CT 2	32	16	12	4	0.667	0.75	0.023
CT 3	48	0	16	0	1	1	0.022
CT 4	48	0	16	0	1	1	0.019
OCT 1	48	0	16	0	1	1	0.022
OCT 2	48	0	16	0	1	1	0.022
CCVT 1	48	0	16	0	1	1	0.021
CCVT 2	48	0	16	0	1	1	0.021
CCVT 3	48	0	16	0	1	1	0.021
CCVT 4	48	0	16	0	1	1	0.021

Table 6.10: Overcurrent Decision Element, AG Fault

Model	N_1	F_1	N_2	F_2	s_1	s_2	$t[s]$
Referent	48	0	16	0	1	1	0.009
CT 1	48	0	16	0	1	1	0.01
CT 2	43	5	9	7	0.896	0.563	0.012
CT 3	48	0	16	0	1	1	0.009
CT 4	48	0	13	3	1	0.813	0.012
OCT 1	48	0	16	0	1	1	0.009
OCT 2	48	0	16	0	1	1	0.009
CCVT 1	48	0	16	0	1	1	0.009
CCVT 2	48	0	16	0	1	1	0.009
CCVT 3	48	0	16	0	1	1	0.009
CCVT 4	48	0	16	0	1	1	0.009

Table 6.11: Overcurrent Decision Element, AG Fault

Model	N_1	F_1	N_2	F_2	s_1	s_2	$t[s]$
Referent	48	0	16	0	1	1	0.024
CT 1	48	0	16	0	1	1	0.028
CT 2	32	16	16	0	0.667	1	0.059
CT 3	48	0	16	0	1	1	0.025
CT 4	48	0	13	3	1	1	0.046
OCT 1	48	0	16	0	1	1	0.024
OCT 2	48	0	16	0	1	1	0.024
CCVT 1	48	0	16	0	1	1	0.024
CCVT 2	48	0	16	0	1	1	0.024
CCVT 3	48	0	16	0	1	1	0.024
CCVT 4	48	0	16	0	1	1	0.024

6.2.2.2 IED Model B

Output signals from the measuring element of the IED model B were not available (there is no access to the output as the model has been previously implemented). Only decision-making element was evaluated. Evaluation results are given in Tables 6.12 through 6.14.

Table 6.12: Distance Decision Element, ABCG Fault

Model	N_1	F_1	N_2	F_2	s_1	s_2	$t_1[s]$	$t_2[s]$
Referent	32	0	28	4	1	0.875	0.017	0.043
CT 1	32	0	32	0	1	1	0.018	0.043
CT 2	32	0	0	32	1	0	0.016	-1
CT 3	32	0	32	0	1	1	0.018	0.043
CT 4	32	0	0	32	1	0	0.015	-1
OCT 1	32	0	32	0	1	1	0.017	0.043
OCT 2	32	0	32	0	1	1	0.017	0.043
CCVT 1	32	0	28	4	1	0.875	0.017	0.043
CCVT 2	32	0	32	0	1	1	0.017	0.043
CCVT 3	32	0	28	4	1	0.875	0.017	0.043
CCVT 4	32	0	28	4	1	0.875	0.017	0.043

Table 6.13: Distance Decision Element, AG Fault

Model	N_1	F_1	N_2	F_2	s_1	s_2	$t_1[s]$	$t_2[s]$
Referent	32	0	32	0	1	1	0.035	0.043
CT 1	24	8	32	0	0.75	1	0.039	0.043
CT 2	17	15	32	0	0.531	1	0.035	0.043
CT 3	32	0	32	0	1	1	0.036	0.043
CT 4	20	12	32	0	0.625	1	0.037	0.043
OCT 1	32	0	32	0	1	1	0.036	0.043
OCT 2	32	0	32	0	1	1	0.036	0.043
CCVT 1	32	0	32	0	1	1	0.034	0.043
CCVT 2	32	0	32	0	1	1	0.035	0.043
CCVT 3	32	0	32	0	1	1	0.034	0.043
CCVT 4	32	0	32	0	1	1	0.034	0.043

Table 6.14: Distance Decision Element, BC Fault

Model	N_1	F_1	N_2	F_2	s_1	s_2	$t_1[s]$	$t_2[s]$
Referent	32	0	28	4	1	0.875	0.017	0.043
CT 1	32	0	32	0	1	1	0.018	0.043
CT 2	32	0	8	24	1	0.25	0.017	0.04
CT 3	32	0	32	0	1	1	0.018	0.043
CT 4	32	0	14	18	1	0.438	0.017	0.04
OCT 1	32	0	32	0	1	1	0.017	0.043
OCT 2	32	0	32	0	1	1	0.017	0.043
CCVT 1	32	0	28	4	1	0.875	0.017	0.043
CCVT 2	32	0	32	0	1	1	0.017	0.043
CCVT 3	32	0	28	4	1	0.875	0.017	0.043
CCVT 4	32	0	28	4	1	0.875	0.017	0.043

6.3 Assessment of Improved Transient Response

6.3.1.1 IED Model A

Performance of the current measuring algorithm (Table 6.3-6.5)

The following conclusion can be made based on results:

- Influence on settling time is negligible
- Influence on overshoot shows significant variations with different instrument transformer models. Current transformer model 2 caused overshoot several times smaller than the overshoot caused by the referent instrument transformer. This is an indication of current transformer saturation (in large number of test cases). Current transformer model 4 caused an overshoot just slightly larger than model 2, while other models caused overshoot similar to the referent.
- Influence on normalized error index shows significant variations. Largest error was produced by model 2. The range of error caused by model 2 is from 30 to 56 percent. Probable cause is the current transformer saturation. Model 4 caused smaller error, in the vicinity of 16 percent, while other models caused low error levels.

- Influence on DC gain shows that model 2 suppressed DC component better than any of the rest of models. Since it was pointed out that model 2 went through saturation in significant number of test cases, it can be concluded that saturation actually enhances suppression of DC component.
- Influence on aggregated frequency index is negligible.

Performance of the voltage measuring element algorithm (Table 6.6-6.8)

The following conclusion can be made based on results:

- Influence on settling time is negligible
- Influence on overshoot varies. Models 2 and 4 caused significantly higher overshoot, compared to other models. Probable cause is inductive nature of burden connected to models 2 and 4. Overshoot caused by other models is slightly higher than overshoot cause by referent model.
- Influences on normalized error index, DC gain and aggregated frequency index are negligible.

Performance of the decision-making algorithm (Table 6.9-6.11)

The following conclusion can be made based on results:

- CT model 2 caused the poorest performance of IED model. Detection of ABCG faults is impacted the most, while AG and BC faults are detected slightly better. The influence of CT model 2 is degrading the IED model performance to unacceptable levels in case of all three faults. The reason for this large measurement error is identified by performance indices of current measuring algorithm. The other model showed no influence on decision making element of IED model A. The CT model 4 did lower selectivity of IED model in backward zone slightly. There is virtually no difference in performance of IED model A when supplied with signals coming from the referent IT (ideal) or Optical CT models

6.3.1.2 IED Model B

The following conclusions can be made based on results (Table 6.12-6.14):

- IED model shows small overreach for ABCG and BC fault types (selectivity in zone 2 is 87.5 percent). However, IED model B showed no overreach effects when connected to CT models 1, 3, Optical CT model 1, Optical CT model 2, and CCVT model 2. This seemingly "positive" influence of IT models is actually masking the problematic performance of IED model. CT models 2 and 4 caused

IED model to overreach complete zone 2 for ABCG fault type. The reason for this is larger error in measurement, caused by mentioned CT models.

6.4 Conclusion

Results of evaluation of transient response of conventional instrument transformers are presented in this section. It was shown how choice of criteria can be used for detection of instrument transformer saturation. Practical, numerical values have been illustrated. Conclusion is that the simulation environment can be used to obtain the results.

7. Assessment Using Field Recorded Data

7.1 Introduction

Evaluation of operation data provided by AEP is presented in this section. First, the sources of field data are discussed. Next, evaluation of data from both the traditional and optical measurement systems have been carried out taking into consideration two main characteristics: transient response and accuracy. Data collected from distance relays located in the field have been corroborated using simulation environment. Simulation environment has also been used in combination with data from DFR to evaluate accuracy of both systems from a power quality perspective.

7.2 Sources of Field Recorded Data

Three sources of field-recorded data that were available for this project:

- ION84000 meter. This IED recorded the following data:
 - True RMS 3-phase voltage, current and power
 - Instantaneous 3-phase voltage, current, frequency, power factor
 - Bi-directional, absolute, net, time-of-use, loss compensation energy
 - Rolling block, predicted, thermal demand
 - Individual, total harmonic distortion up to the 63rd harmonic
 - Sag/Swell
 - Number of Nines (power availability)
 - Symmetrical components
 - K-Factor for voltage and current inputs

The mentioned data was accessible through remote, dial-up connection, using ION software.

- TESLA recorder. This IED is a digital fault recorder (DFR). It captures current and voltage signals for a period of time, when triggered by a certain event. Recorded data was accessible through remote, dial-up connection, using TESLA access software.
- Distance Relays: SEL 321, GE D60. Event records, fault reports and oscillography were available for each event seen by the relays. Records were retrieved in the form of Comtrade files. Some of the available data was:

- Fault Location
- Fault Type
- Protection function that operated
- Tripping time
- Date and time of fault

Figure 7.1 shows the field connections of the described equipment for the optical instrument transformer evaluation on the 345kV Kirk line exit at AEP's Corridor Station.

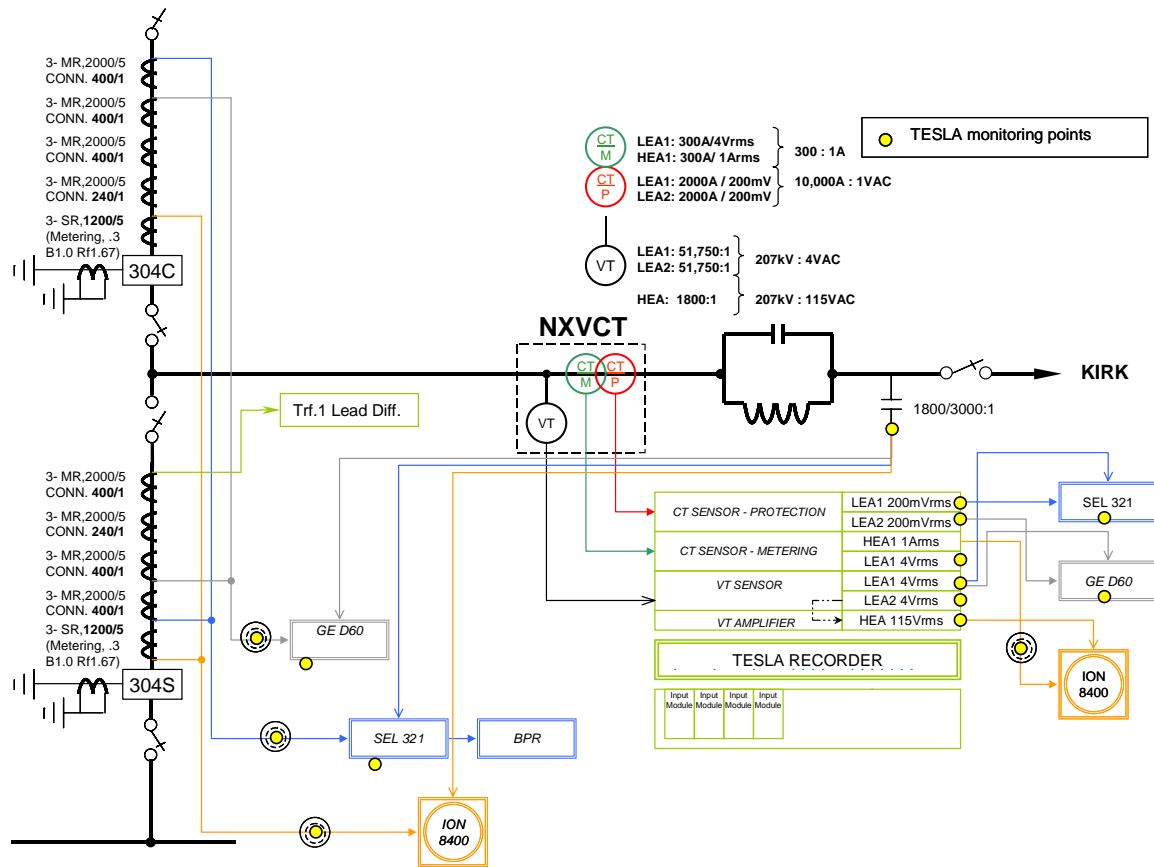


Fig. 7.1: Setup for Field Data Recording

7.3 Evaluation of Transient Response

The transient response of the novel protection system (using optical ITs) was measured with respect to its influence on the relay performance. The use of field data imposes inherent limitations, among these restrictions the most important one is a small number of events available for the analysis. A total of 7 events were recorded by both the SEL-321 and GE D60 relays. Data collected from each event are shown in Table 7.1.

Evaluation Results

- Influence of the optical measurement system on the relay's tripping time was negligible. There was a difference in only 2 out of 7 recorded events with an average percent difference of 3.9.
- Influence of the optical measurement system on the relay's fault location calculation was also negligible for the one event in which the distance protection function picked up. The percent difference was 2.45 for the SEL 321 and 3.23 for the GE D60.

Table 7.1: Relay – Field Recorded Data.

Event Date	Protection Function	Fault type	Tripping Time [sec]		Fault Location			
			GE D60		SEL 321		GE D60	
			Conv IT	Opt IT	Conv IT	Opt IT	Conv IT	Opt IT
3/25/05	Distance Z1	BG	0.0323	0.0323	11.71	11.43	12.4	12.8
10/28/04	Neg. Seq. Dir. OC	BG	0.0318	0.0333				
8/23/04	Neg. Seq. Dir. OC	BG	0.0323	0.0323				
7/1/04	Neg. Seq. Dir. OC	BG	0.0323	0.0333				
5/26/04	Neg. Seq. Dir. OC	CG	0.0323	0.0333				
5/21/04	Neg. Seq. Dir. OC	CG	0.0318	0.0318				
5/17/04	Neg. Seq. Dir. OC	AG	0.0323	0.0323				

Note: Conv IT denotes that relay was supplied by signals coming from conventional instrument transformers. Opt IT denotes that a relay was supplied by signals coming from optical instrument transformers. SEL 321 was not programmed for the Neg. Seq. Dir. OC protection function

7.4 Evaluation of Accuracy

The accuracy of the novel protection system (using optical ITs) was measured with respect to its influence on power quality meter performance. Focus will be placed on the influence on PQ meter (IED model C) to correctly detect and characterize voltage sags (short duration reductions in rms voltage). The same procedure used for the assessment of higher accuracy through simulation has been utilized to analyze the available field data. The PQPI served then as an indicator of the difference in PQ meter performance when supplied with signals from either the conventional or the optical ITs. Data recorded through the TESLA recorder was available for 16 voltage sags. These events were processed and stored into database of exposures to be replayed to IED model C via simulation. Results for calculated power quality performance indices (PQPI) can be found in table 7.2:

Table 7.2: Power Quality Performance - 16 Recorded Sags

Model	Detection Method	Sag/Swell Characterization	
	PQPI - Detection	PQPI - Duration	PQPI - Average RMS
Sag	0	0.0014	0.0007

Evaluation Results

- Influence of the optical measurement system on the PQ meter model's ability to properly detect voltage sags was negligible. For all recorded sags both the novel measurement system (PQ meter model with signals from optical IT) and the conventional measurement system (PQ meter model with signals from conventional IT) were able to detect and characterize the voltage sag.
- Influence of the optical measurement system on the PQ meter's sag duration and average RMS estimation was also negligible. The PQPI shows a percent difference of 0.14 for the PQPI – duration and 1.59 for the PQPI – Average RMS (considering and mean RMS value of 0.989 pu and mean duration of 0.044 sec)

7.5 Conclusion

Results of evaluation of field data have been presented in this section. It was shown how the criteria implemented by the means of simulation could be combined with field data to quantify the difference in performance between an optical and traditional measurement systems.

8. Conclusion

As explained in section 1, only a model of an optical current transformer was available for this study, hence, an assessment of the influence of optical voltage transformer (OVT) characteristics on the performance of measurement and protection IED has not been performed. The simulation environment offers the flexibility to incorporate models of available OVT in the future by using the same methodology and testing scenarios.

This report has shown that:

- A specific set of criteria can be defined to evaluate accuracy, frequency bandwidth, dynamic range and transient response of instrument transformers (see sections 3, 4 and 5)
- Indirect evaluation methodology can be used to evaluate instrument transformers in the case when primary side (referent) signals are unavailable (see section 3).
- Methodology can be implemented through simulation software (see section 3)
- Numerical performance indices indicative of instrument transformer performance can be defined. The results can be used for comparison of the performance of different instrument transformers (see sections 3, 4 and 5)

The conclusions from this report are:

- Evaluation of the benefits of higher accuracy shows that the better accuracy expected from optical IT does not translate into a significant improvement (see results for PQPI-Average RMS in section 4.3) in the performance of the power quality and/or revenue metering IEDs when compared with the performance of the same devices (represented by IED model C in this study) having conventional IT as input sources.
- Evaluation of the benefits of wider frequency bandwidth shows that the bandwidth of optical instrument transformers will considerably improve the performance, making it possible to use the same set of optical transformers for relaying and metering applications. (Results were produced under the assumption that the optical voltage transformer would have a very large frequency bandwidth; close to ideal, however, no model data was available to confirm this)
- Evaluation of the benefits of better transient response shows that the performance of protection IED models improved when fed with signals from optical current transformers. The reason for this improvement is explained by the absence of CT saturation. It was also recognized that not all the conventional CT models experienced saturation up to the level that would cause misoperation of protection

IED, which suggests that the problem of the impact of saturation on protection IED performance can be avoided even when using conventional IT by proper sizing of the transformers.

- Evaluation using field data shows that the protective relays and power quality meters did not have a significant difference in performance when using optical instrument transformers as input sources. The number and type of events available for analysis from field data was very limited which is why the use of models in the evaluation is preferred so that all possible fault scenarios can be considered.

References

- [1] J. L. Blackburn, "Protective Relaying: Principles and Applications", *Marcel Dekker*, New York, 1998.
- [2] P. M. Anderson, "Power System Protection", *McGraw-Hill*, New York, 1999.
- [3] C. Christos, A. Wright, "Electrical Power System Protection", *Kluwer Academic Publishers*, Boston, 1999.
- [4] IEEE standard C57.13-1993, "IEEE Standard Requirements for Instrument Transformers", *The Institute of Electrical and Electronics Engineers*, New York, 1994.
- [5] M.I. Samesima, J.C. de Oliveira, E.M. Dias, "Frequency Response Analysis and Modeling of Measurement Transformers Under Distorted Current and Voltage Supply", *IEEE Transactions on Power Delivery*, Vol. 6, No. 4, pp. 1762-1768, October 1991.
- [6] D. Tziouvaras, P. McLaren, et al, "Mathematical Models for Current, Voltage and Coupling Capacitor Voltage Transformers", *IEEE Transactions on Power Delivery*, Vol. 15, No. 1, pp. 62-72, January 2000.
- [7] Lj. Kojovic, M. Kezunovic, S.L. Nilsson, "Computer Simulation of a Ferroresonance Suppression Circuit for Digital Modeling of Coupling Capacitor Voltage Transformers", *ISMM Conference on Computer Applications in Design, Simulation and Analysis*, Orlando, March 1992.
- [8] IEEE Power System Relaying Committee Report, "Transient Response of Current Transformers", *The Institute of Electrical and Electronics Engineers*, New York, 1976.
- [9] IEEE Committee Report, "Transient Response of Coupling Capacitor Voltage Transformers", Working Group of the Relay Input Sources Subcommittee of the Power System Relay Committee, *IEEE Transactions on Power Apparatus and Systems*, Vol. PAS-100, No. 12, December 1981.
- [10] IEEE/PSRC Working Group I3, "Transmission Protective Relay System Performance Measuring Methodology", *The Institute of Electrical and Electronics Engineers*, New York, 1999. Available online: <http://www.pes-psrc.org/>.
- [11] Group of authors, *IEEE Std. C57.113-1994: IEEE Standard Requirements for Instrument Transformers*, *The Institute of Electrical and Electronics Engineers*, New York, 1994.
- [12] M. Kezunovic, B. Naodovic, "Task #1 Report: Performance Shortcomings of Conventional Instrument Transformers", *PSERC Project T-22 Report*, Texas A&M University, July 2004.
- [13] Lj. A. Kojovic, "Impact of Current Transformer Saturation on Overcurrent Protection Operation," *IEEE Power Engineering Society Summer Meeting*, Vol. 3, pp. 1078-1083, July 2002.
- [14] H.O. Pascual, J.A. Rapallini, "Behaviour of Fourier, Cosine and Sine Filtering Algorithms for Distance Protection, Under Severe Saturation of the Current Magnetic Transformer," *IEEE Porto Power Tech Proceedings*, Vol. 4, September, 2001.

- [15] M.A. Hughes, "Distance Relay Performance as Affected by Capacitor Voltage Transformers", *Proceedings of IEE*, Vol. 121, No. 12, pp. 1557-1566, December 1974.
- [16] W.D. Humpage, K.P. Wong, "Influence of Capacitor-Voltage-Transformers on the Dynamic Response of Distance Protection," *Electrical Engineering Transactions*, The Institution of Engineerings, Australia, Vol. EE14, No. 2, pp. 59-63, 1978.
- [17] E. A. Udren, J. A. Zipp, "Proposed Statistical Performance Measures for Microprocessor-Based Transmission-Line Protective Relays, Part 1: Explanation of the Statistics," *IEEE Transactions on Power Delivery*, Vol. 12, No. 1, pp. 134-143, January 1997.
- [18] M. Kezunovic, B. Kasztenny, "Design Optimization and Performance Evaluation of the Relay Algorithms, Relays and Protective Systems Using Advanced Testing Tools," *IEEE Transactions on Power Delivery*, Vol. 15, No. 4, pp. 1129-1135, October 2000.
- [19] Power Measurement, ION8400 Features Summary, available online: <http://www.pwrm.com>.
- [20] D. Ristanovic, S. Vasilic, M. Kezunovic, "Design and Implementation of Scenarios for Evaluating and Testing Distance Relays," *North American Power Symposium - NAPS*, College Station, Texas, October 2001.
- [21] D. Tziouvaras, P. McLaren, C. Alexander, D. Dawson, J. Esztergalyos, C. Fromen, M. Glinkowski, I. Hasenwinkle, M. Kezunovic, L. Kojovic, B. Kotheimer, R. Ruffel, J. Nordstrom, S. Zochol, "Mathematical Models for Current, Voltage and Coupling Capacitor Voltage Transformers," *IEEE Transactions on Power Delivery*, Vol. 15, No. 1, pp. 62-72, January 2000.
- [22] R. C. Dugan, M. F. McGranaghan, H. W. Beaty, *Electrical power systems quality*, McGraw-Hill, New York, 1996.

Appendix – Published Conference Papers

- [1] M. Kezunovic, B. Naodovic, "A Methodology for Assessing the Influence of Instrument Transformer Characteristics on Power System Protection Performance", *Power Systems Computation Conference*, Liege, Belgium, 2005.
- [2] M. Kezunovic, L. Portillo, G. Karady. Sadik Kucuksari, "Impact of Optical Instrument Transformer Characteristics on the Performance of Protective Relays and Power Quality Meters", *IEEE T&D Latin America*, Caracas, Venezuela, 2006.